Geophysics:

From Fundamentals to Recent Studies and Open Questions

Dr. David Santamaría-Pérez

[1] Departamento de Física Aplicada - ICMUV, MALTA Consolider Team, Universitat de València, Spain

***Author E-mail:** David.Santamaria@uv.es

Outline

- ✓ Introduction.
- ✓ Experimental methodology for HP-HT measurements
- ✓ Structure and composition of the Earth's interior
  - The crust
  - The mantle
  - The core
- ✓ Open questions and recent HP-HT studies
  - Earth's core: Light elements, solid and liquid phases, etc.
  - Phase transitions in the Earth's mantle. Properties of materials at high densities.
  - Deep carbon cycle
  - Hydrogen metallization and gas-giant planets

Knowledge of Earth's inner structure

- Seismic waves. They depend on:
  - the composition
  - the mineral phase
  - the density
- Gravitational and magnetic Earth fields
- Flow of heat from inside the Earth
- Composition of meteorites and surface rocks
- Laboratory experiments (High-pressure and high-temperature)

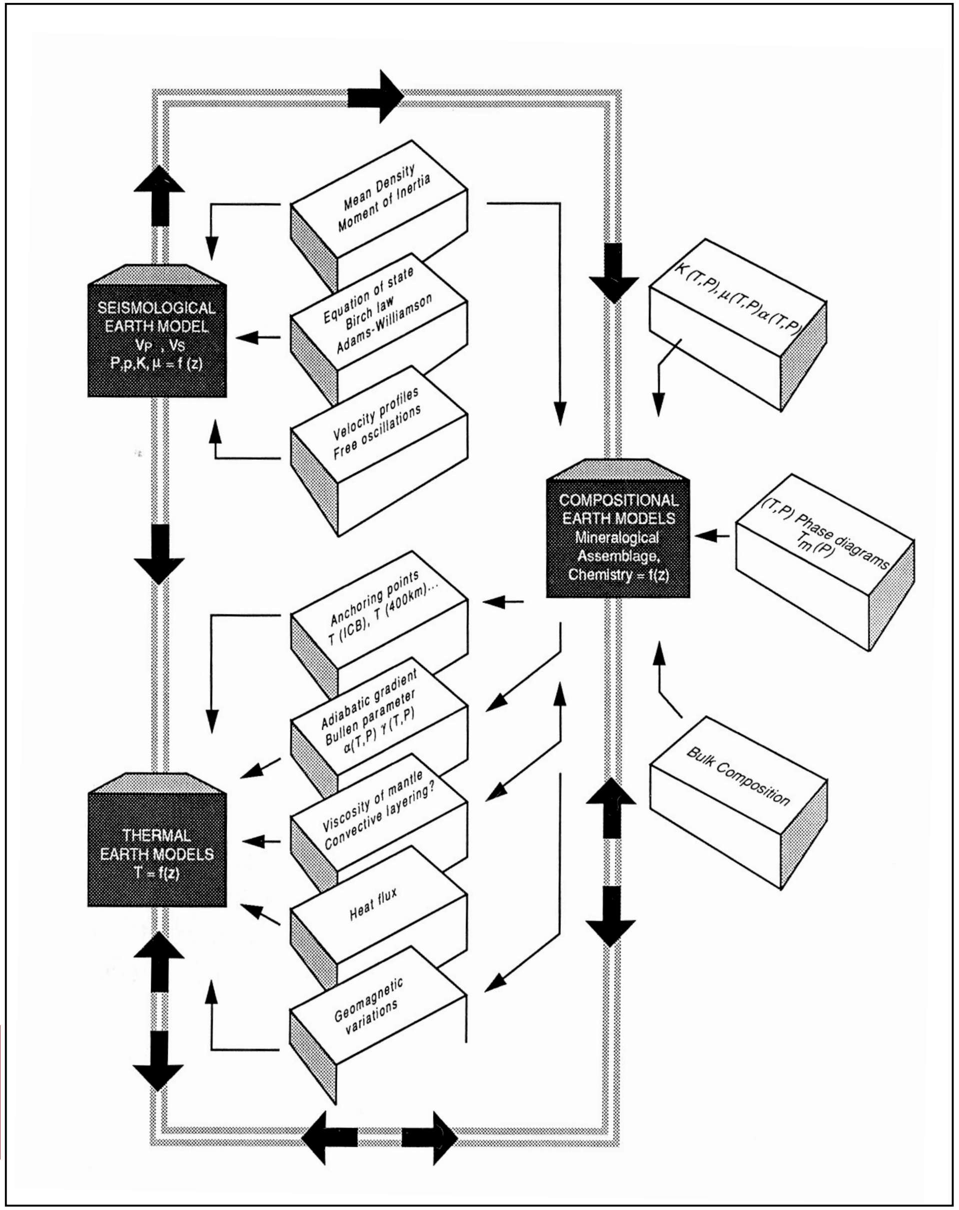

J.P. Poirier (2000)

Earth's interior

- Discontinuities determined from analyses of seismic waves

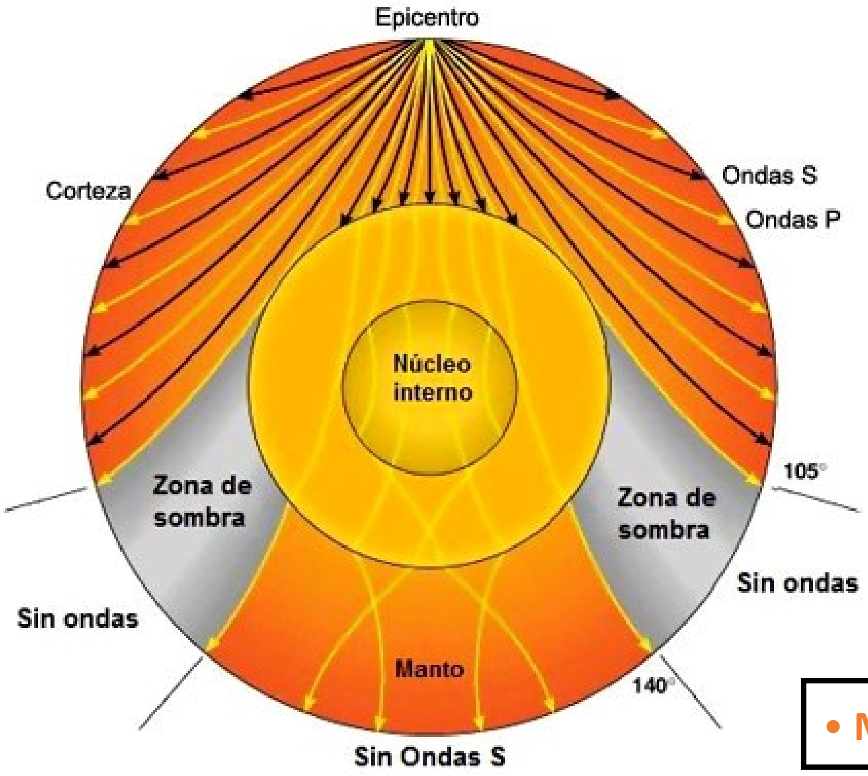

$$V_P = \sqrt{\left(K + \frac{4}{3}\mu\right) / \rho}$$

$$V_S = \sqrt{\frac{\mu}{\rho}}$$

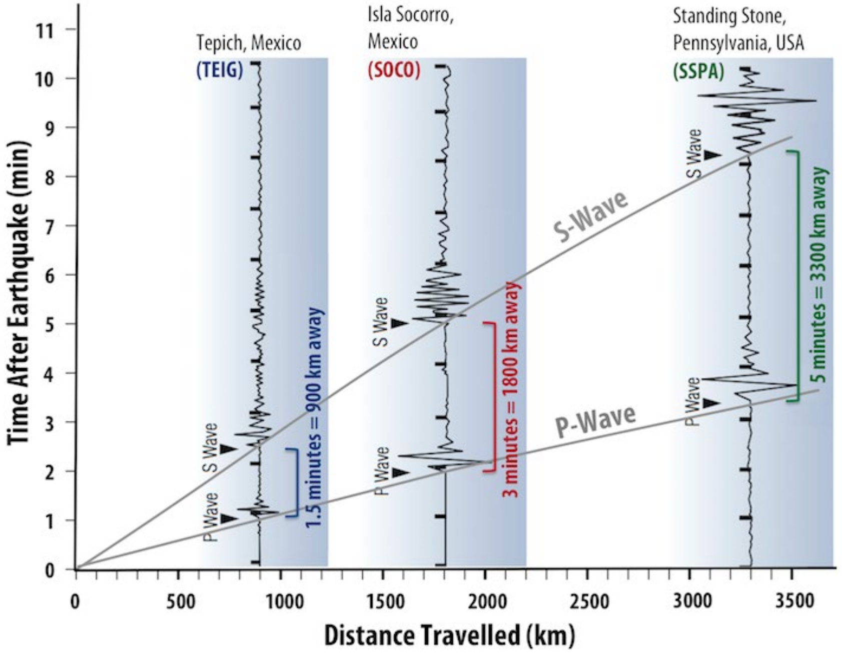

Earth's core

- Mainly composed of iron

- Liquid outer core
- Solid inner core

Heat flow

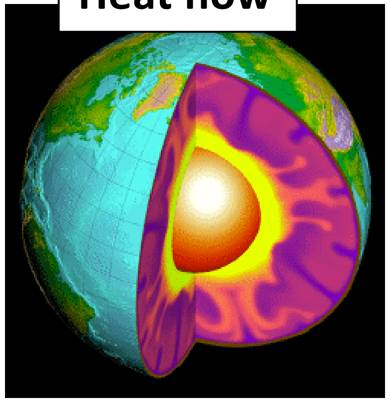

Magnetic field

HP-HT experimental techniques

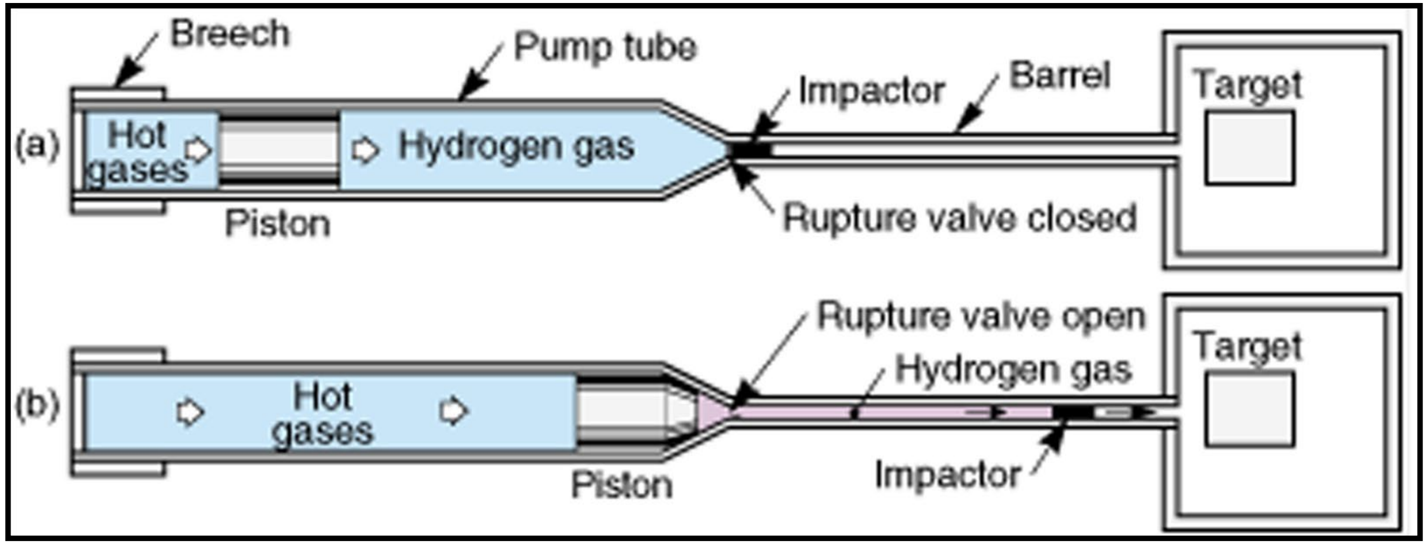

DYNAMIC PRESSURE

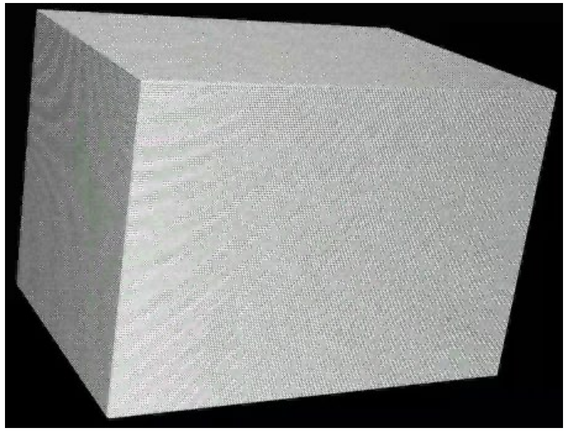

Shock waves

- Produced by impact of high-velocity projectiles
- Extreme conditions (HP – HT) during periods of ~ 1μs

HP-HT experimental techniques

Sample volumes up to 0.1 cm^3.
$V_{LAC} >>> V_{DAC}$

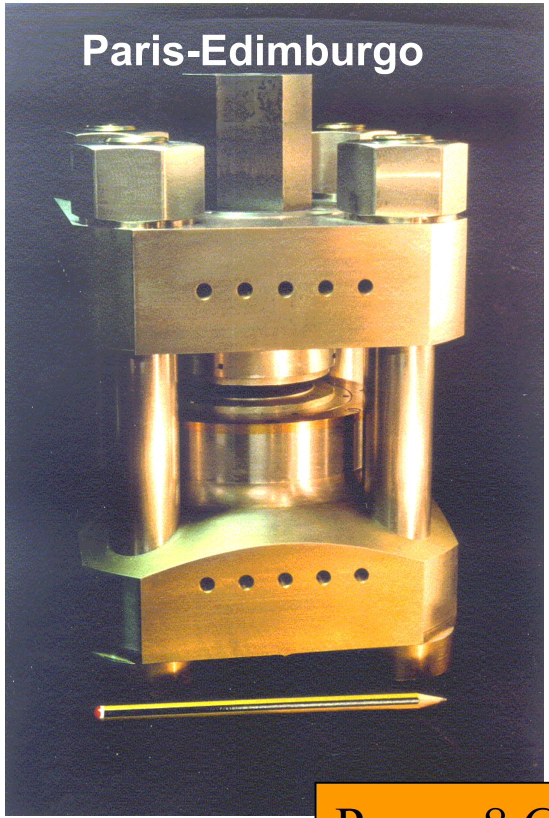

$P_{max} = 8$ GPa
$T_{max} = 2000$ K

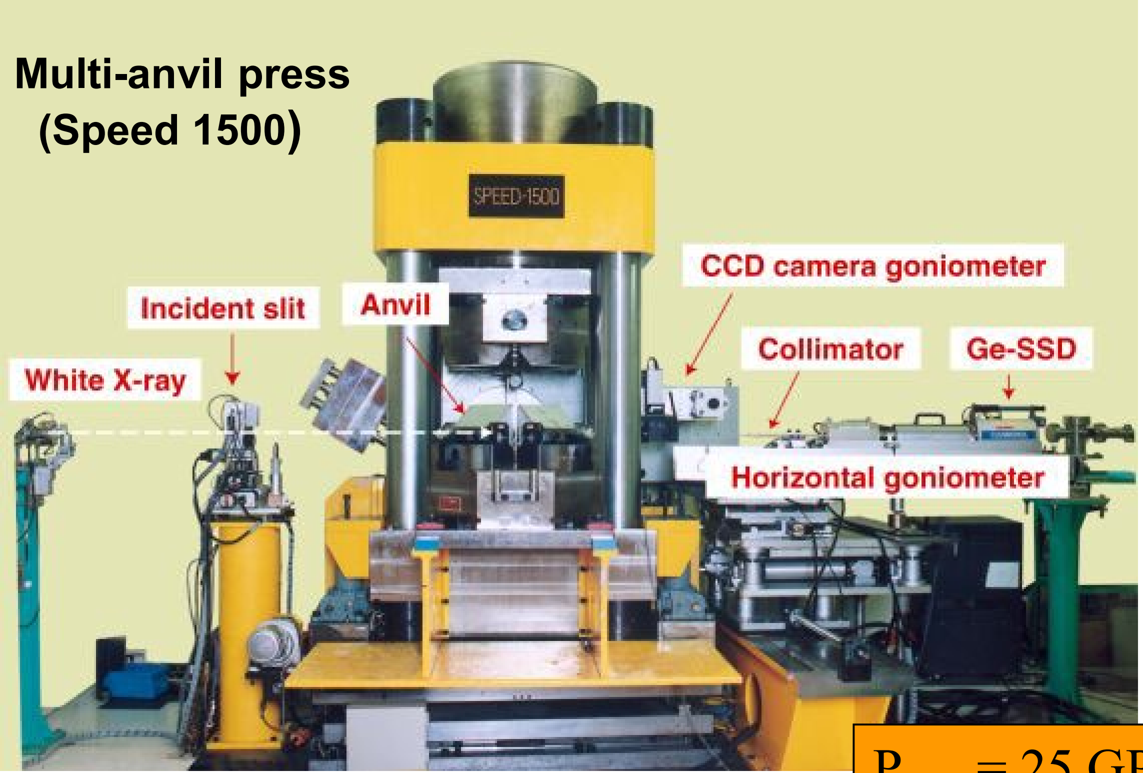

$P_{max} = 25$ GPa
$T_{max} = 2300$ K

LARGE VOLUMEN PRESSES

HP-HT experimental techniques

Diamond anvil cells (DACs)

DIAMOND
- **Hardness**
- **Thermal conductivity**
- **Good optical windows**

$P_{max} = 250$ GPa
$T_{max} = 5500$ K

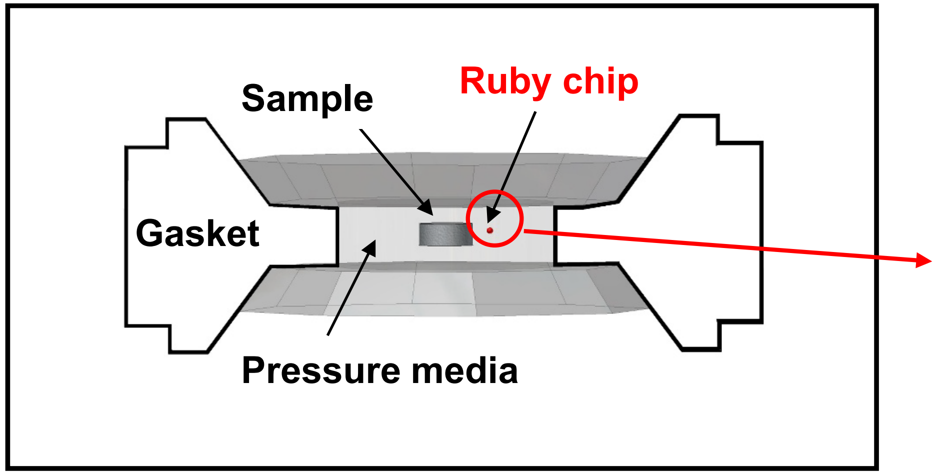

Pressure chamber

Tiny samples: 20 μm x 20 μm x 5 μm

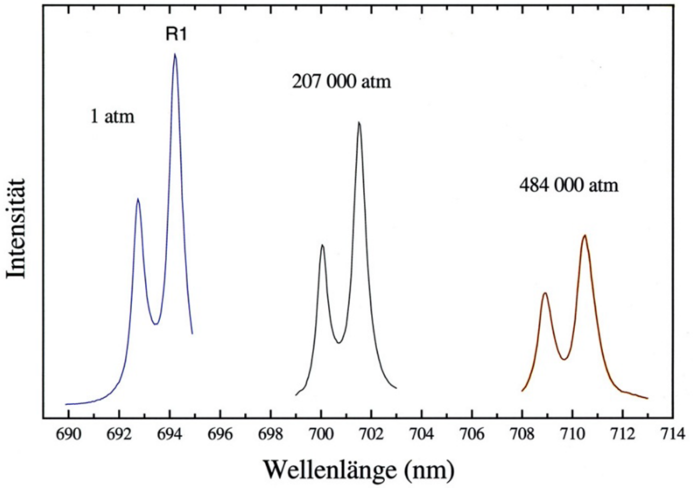

R1 and R2 fluorescence peaks of ruby with pressure

HP-HT experimental techniques

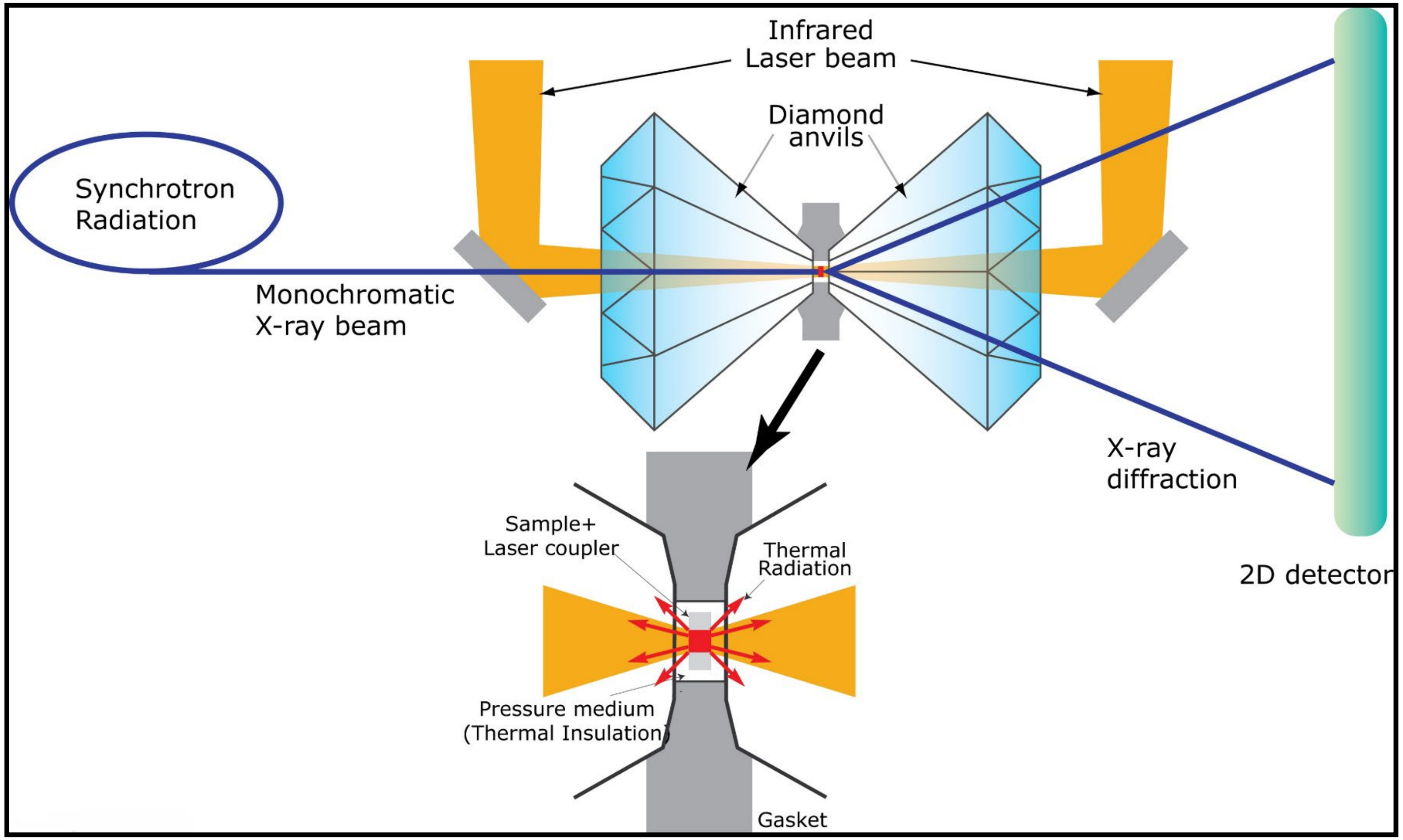

DOUBLE-SIDED LASER HEATING

HP-HT experimental techniques

LASER HEATING AND TEMPERATURE MEASUREMENTS

$$I(\lambda) = \frac{\varepsilon c_1 \lambda^{-5}}{e^{c_2/\lambda T} - 1}$$

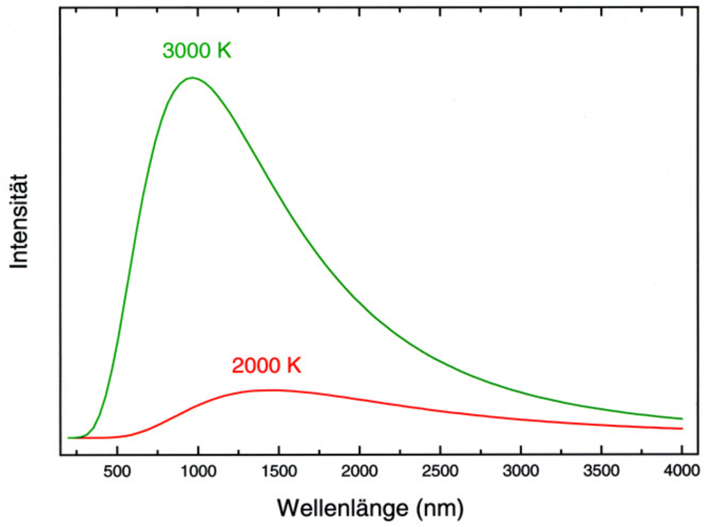

Emmision spectra at 2000 y 3000 K.

1. Center of the hotspot (areas of 2 μm diameter)
2. Fitting Planck equation to the spectra
   - Wavelength-independent emissivity

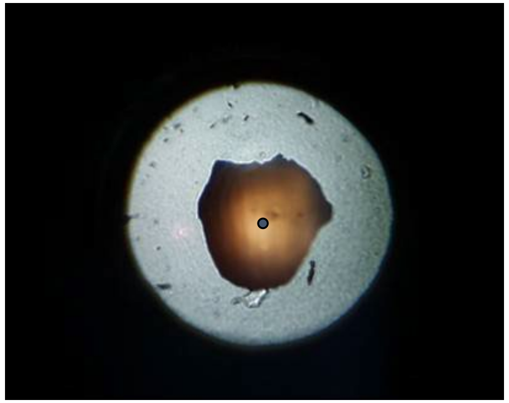

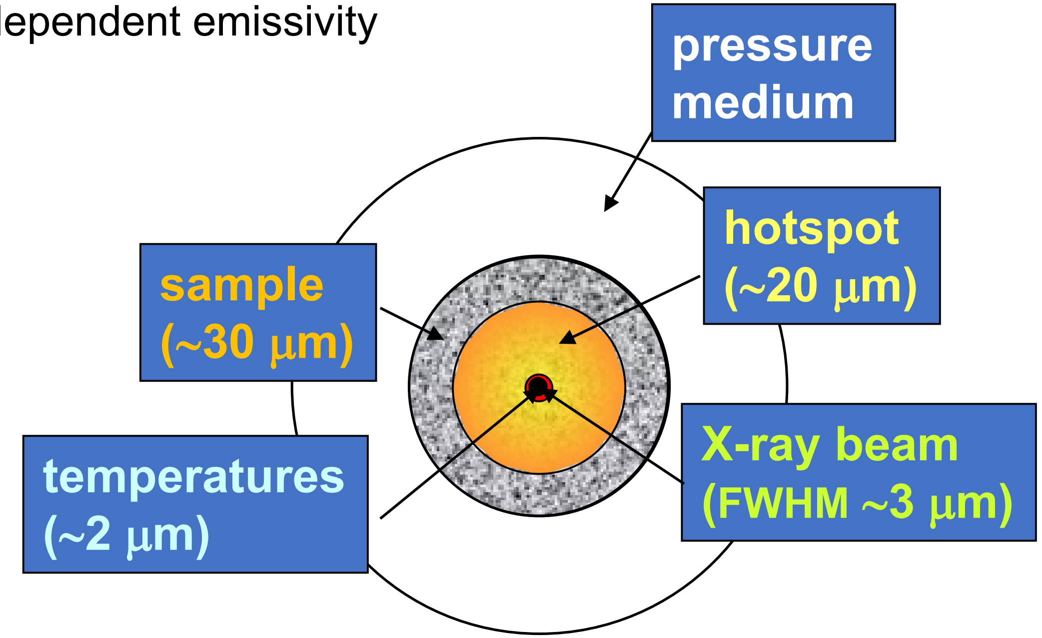

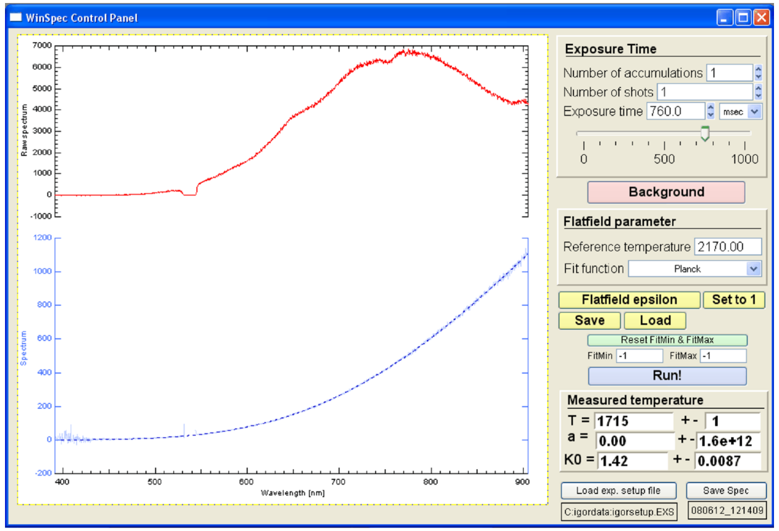

Example of temperature fitting

HP-HT experimental techniques

SYNCHROTRON RADIATION

APS (Advanced Photon Source), Chicago, USA.

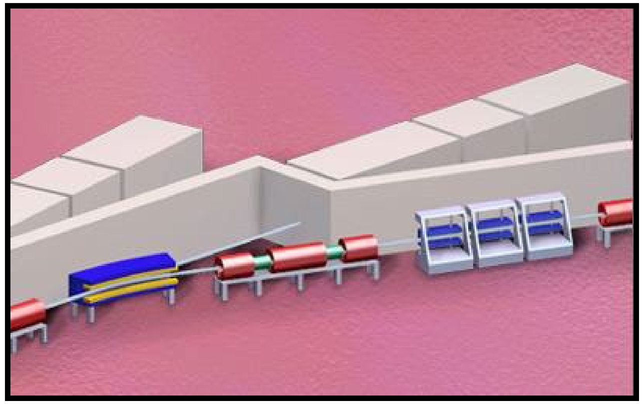

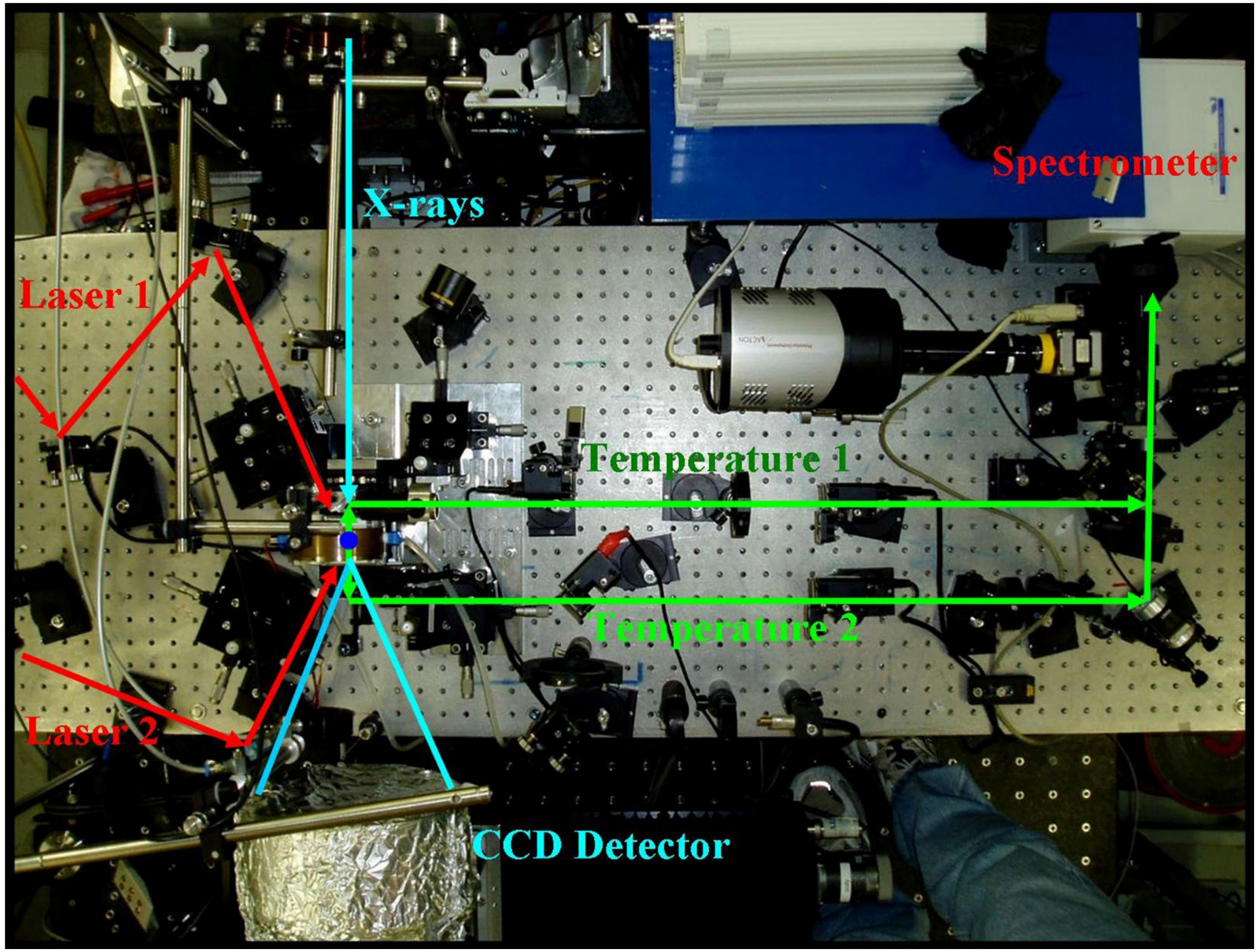

Double-sided DAC laser heating system, ID27 (ESRF), Grenoble, France.

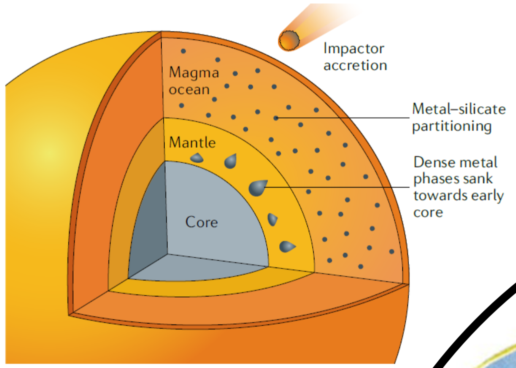

Early Earth accretion, metal segregation and core formation (>4.5 Ga)

Earth's interior

Today

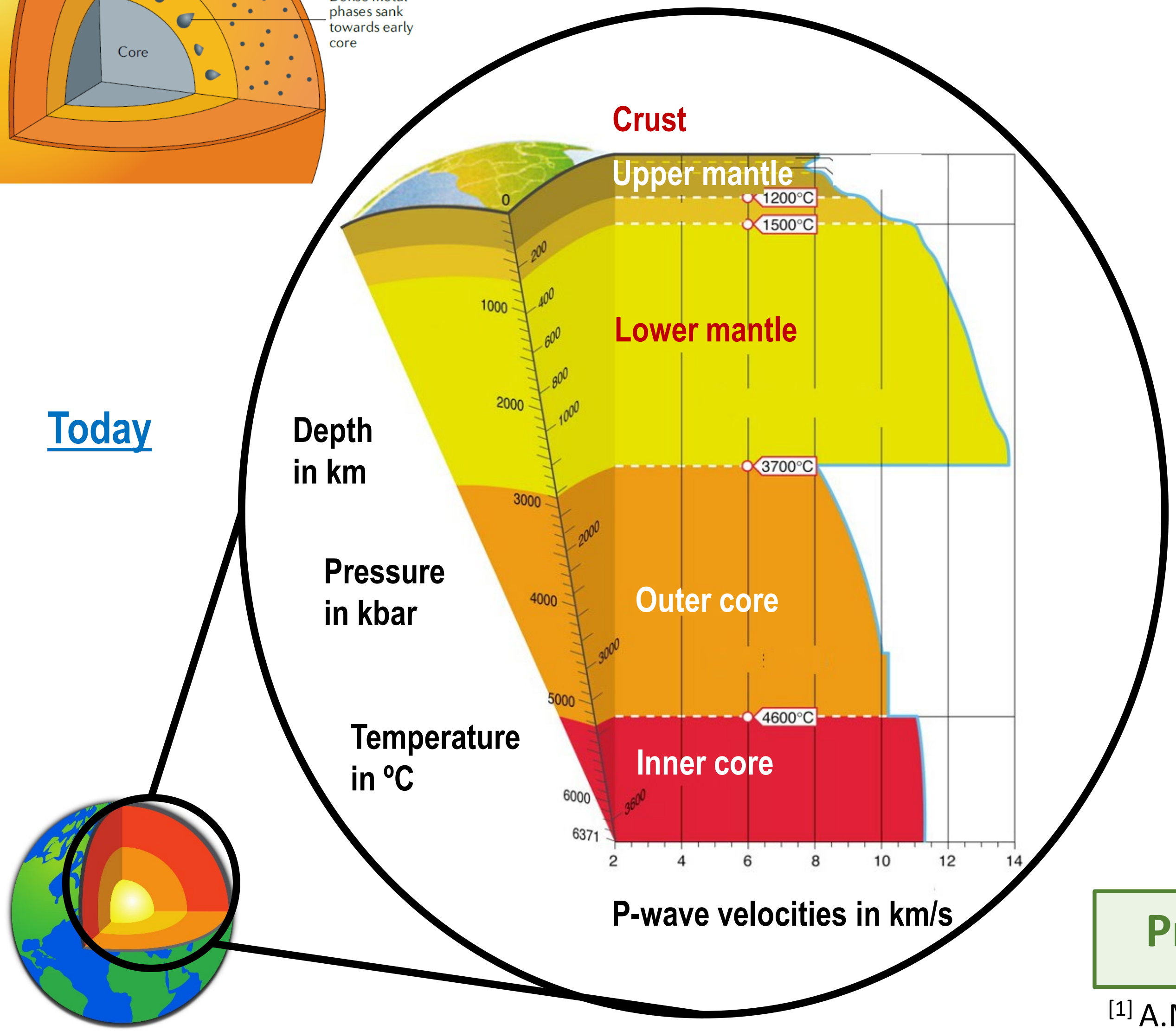

Crust

Heterogeneous rocks. e.g. quartz, feldspars, micas, olivine, calcite, hornblende, etc...

Upper mantle

Piroxene, olivine

Intermediate mantle (transition zone)

Garnet, spinel

Lower mantle

Perovskite, post-perovskite

Core

Fe + 5 % Ni + 5-10 % lighter elements

Preliminary Reference Earth Model (PREM)

[1] A.M. Dziewonski, D.L. Anderson (1981) Phys. Earth. Planet. Int., 25, 297

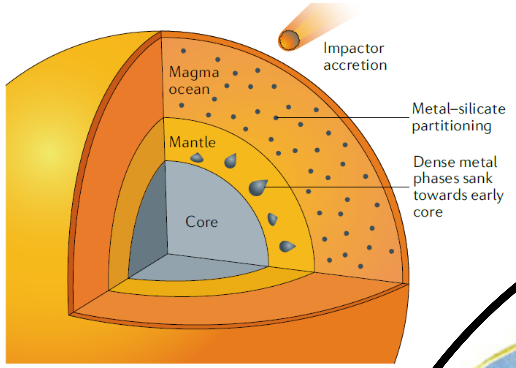

Early Earth accretion, metal segregation and core formation (>4.5 Ga)

Earth's interior

Today

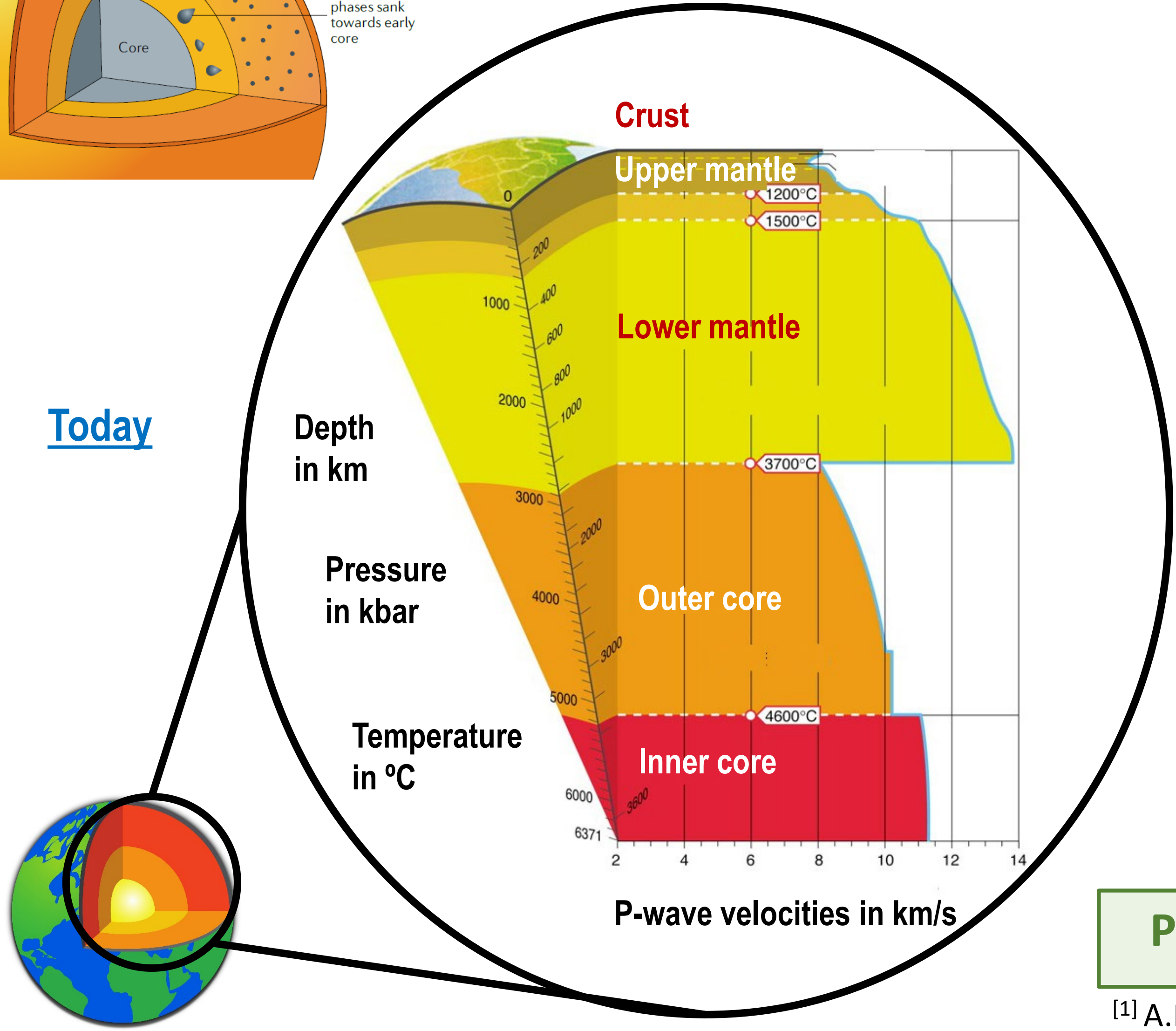

Crust

Heterogeneous rocks. e.g. quartz, feldspars, micas, olivine, calcite, hornblende, etc...

Upper mantle

Piroxene, olivine

Intermediate mantle (transition zone)

Garnet, spinel

Lower mantle

Perovskite, post-perovskite

Core

Fe + 5 % Ni + 5-10 % lighter elements

Preliminary Reference Earth Model (PREM)

[1] A.M. Dziewonski, D.L. Anderson (1981) Phys. Earth. Planet. Int., 25, 297

Composition of the Earth's core

SEISMIC DATA

- Outer and inner core: 6-8% and 4-5% less dense than Fe
- 4-5 % P-wave velocity excess compared to Fe

GRAVITATIONAL FIELD

- Earth's moment of inertia

COSMOCHEMISTRY

- Elements depleted in silicate Earth relative to chondrite meteorites
- Volatile elements

Light elements in the core

The core is considered to have ~5 % weight of Ni. (This fact did not affect significantly the density)

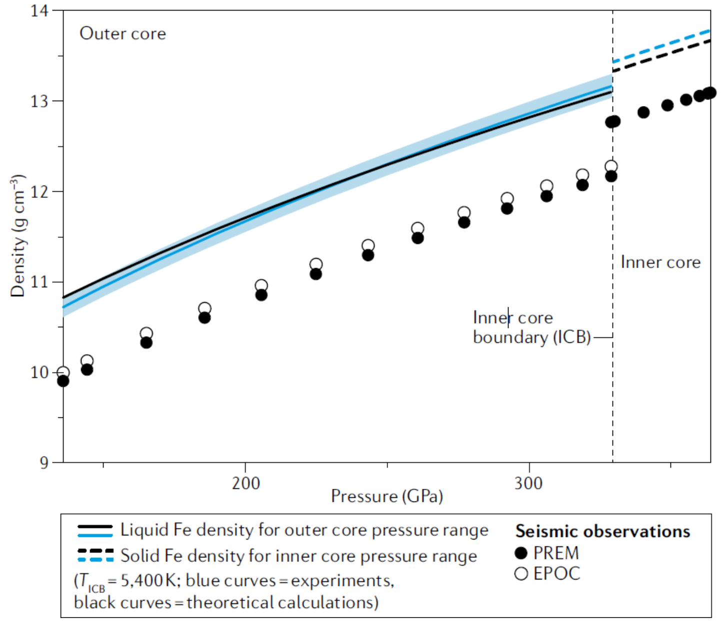

Conditions:

- Lighter than Fe
- Capable of forming alloys with Fe (siderophiles)
- Cosmochemical arguments (Abundance)

~85-90 % weight

Fe 55.85

S 32.07 | **Si** 28.09 | **O** 16.00 | **C** 12.01 | **H** 1.01

[2] F. Birch (1952) J. Geophys. Res. 57, 227-286.
[3] K. Hirose, B. Wood, L. Vocadlo. (2021) Nature Reviews Earth 2, 645–658

Pure iron P-T phase diagram

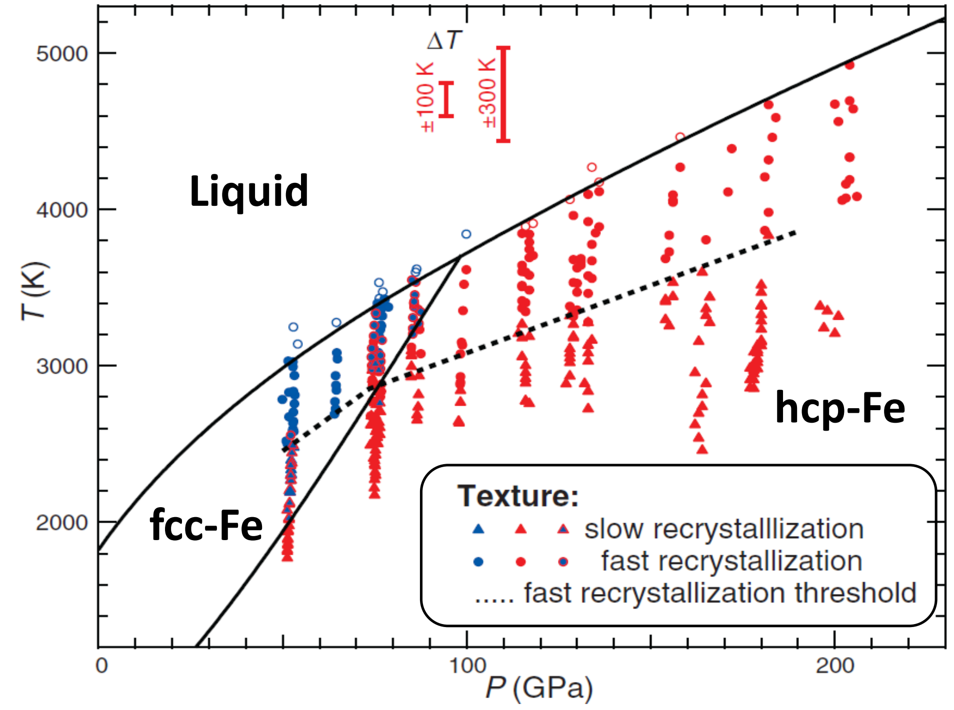

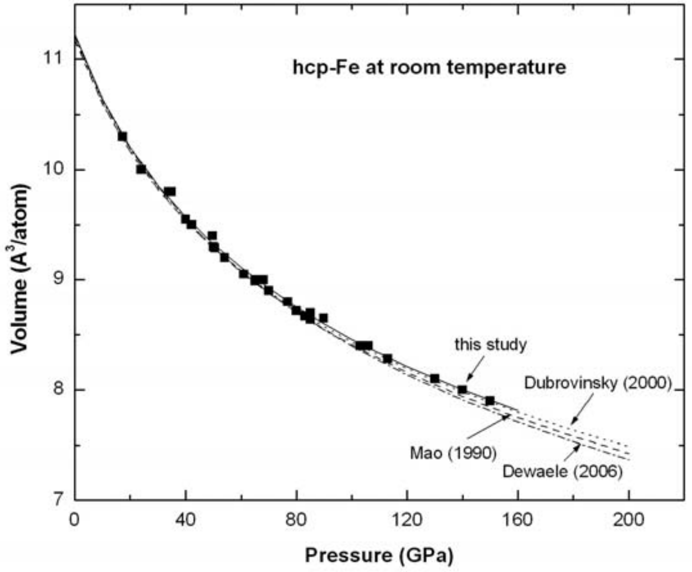

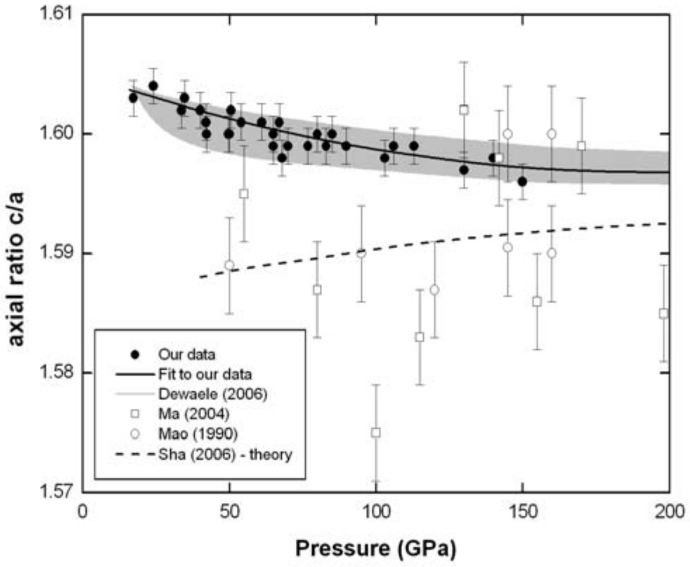

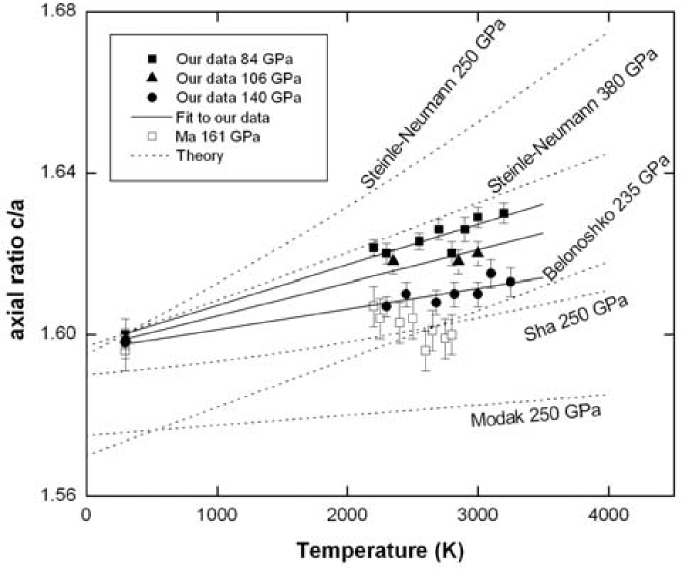

[4] S. Anzellini et al. (2013) Science 340, 464-466
[5] R. Boehler, D. Santamaria-Perez, et al. (2008) J. Phys. 121, 022018

[6] L. Dubrovinsky et al. (2007) Science 316, 1880-1883
[7] Z. Li, D. S. Scandolo (2025) Nature Commun. 16, 7574
[8] D. Ikuta et al. (2021) Commun. Earth Environ. 2, 225

New HP-HT phase of Fe-Ni alloy

P = 225 GPa
T = 3100 K

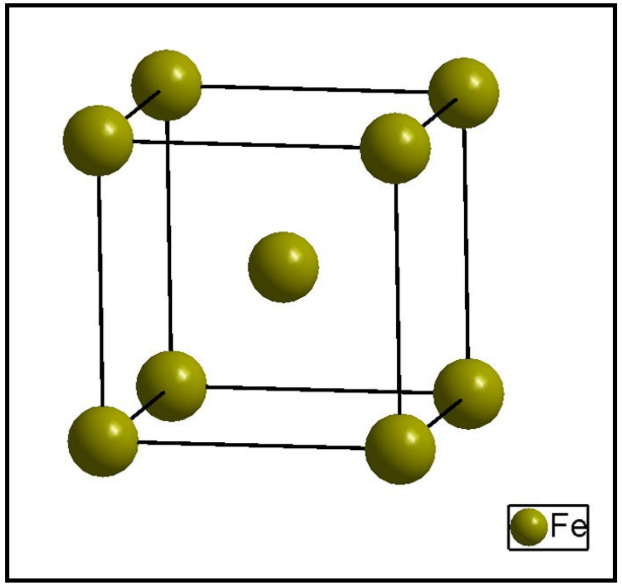

$Fe_{0.9}Ni_{0.1}$

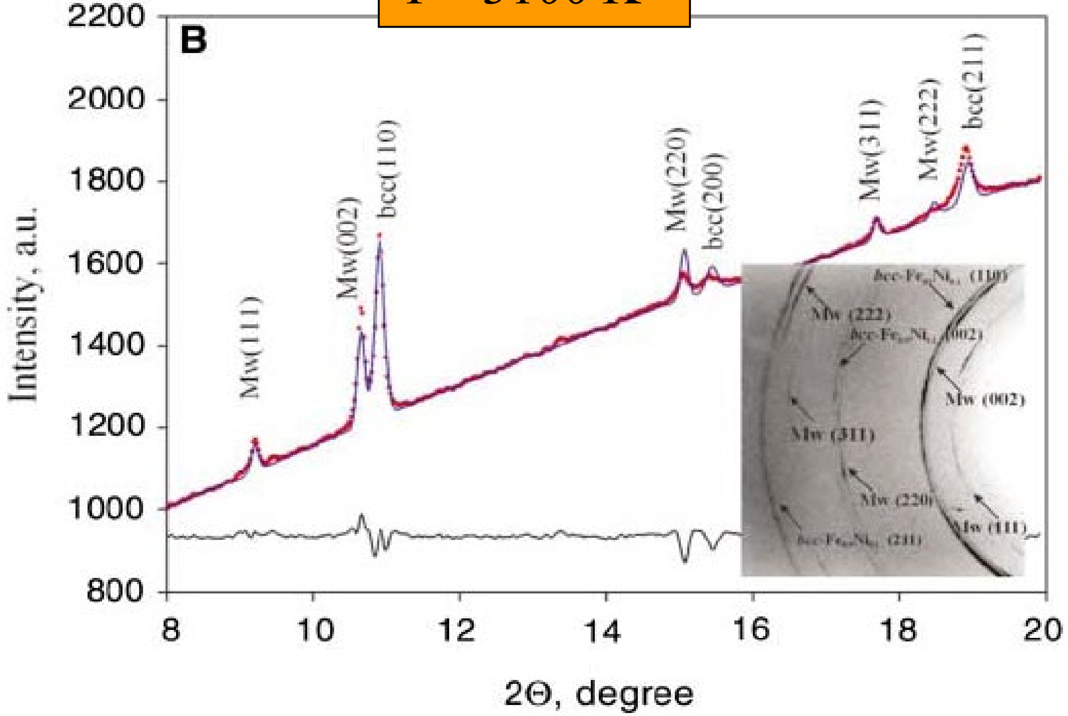

$Fe_{0.83}Ni_{0.07}Si_{0.10}$

Body-Centered Cubic Iron-Nickel Alloy in Earth's Core

Article

https://doi.org/10.1038/s41467-025-62666-1

Short-range order stabilizes a cubic iron alloy in Earth's inner core

Liquid iron alloys at HP and HT

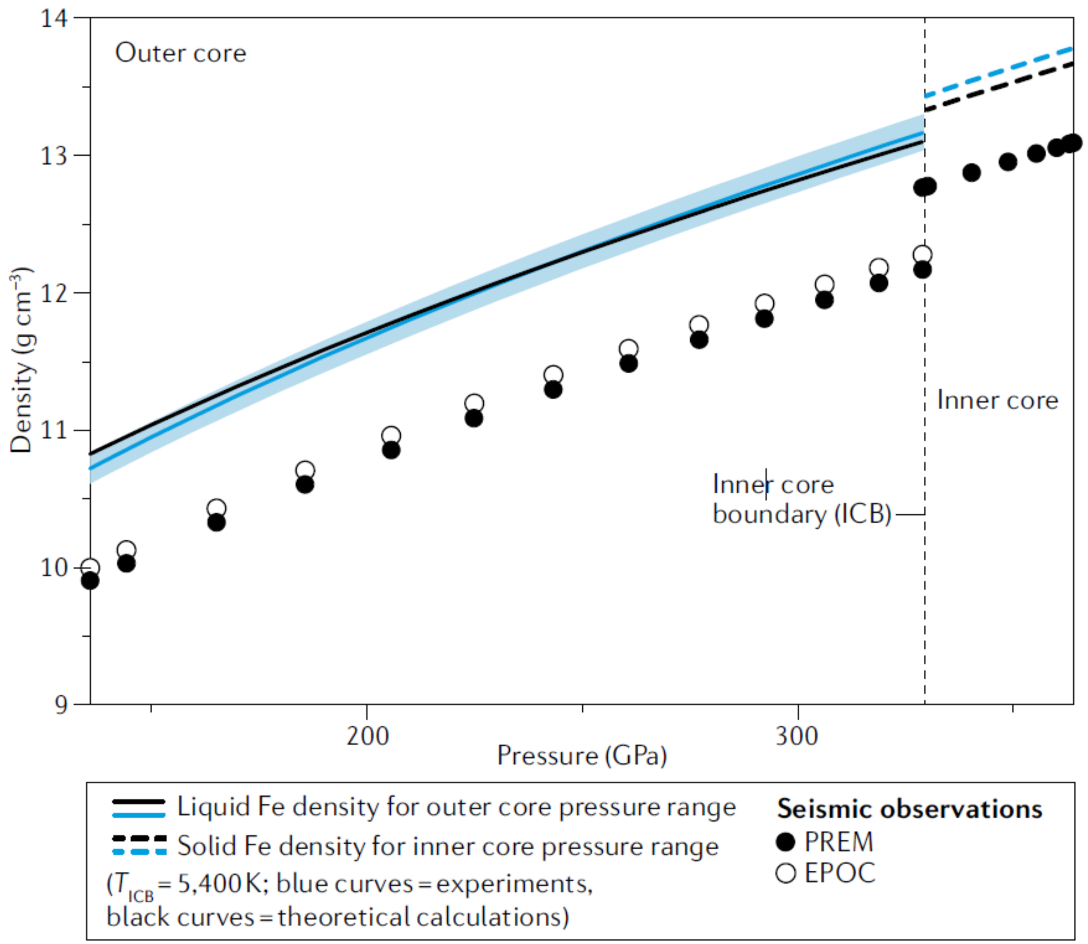

Data from:

[3] K. Hirose, B. Wood, L. Vocadlo. (2021) Nature Reviews Earth 2, 645–658

[9] G. Morard et al. (2013) Earth Planet Sci. Lett. 373, 169-178

[10] D. Santamaría-Perez, R. Boehler (2008) Earth Planet Sci. Lett. 265, 743-747

[11] D. Huang et al. (2026) Nature Commun. 16, 7574

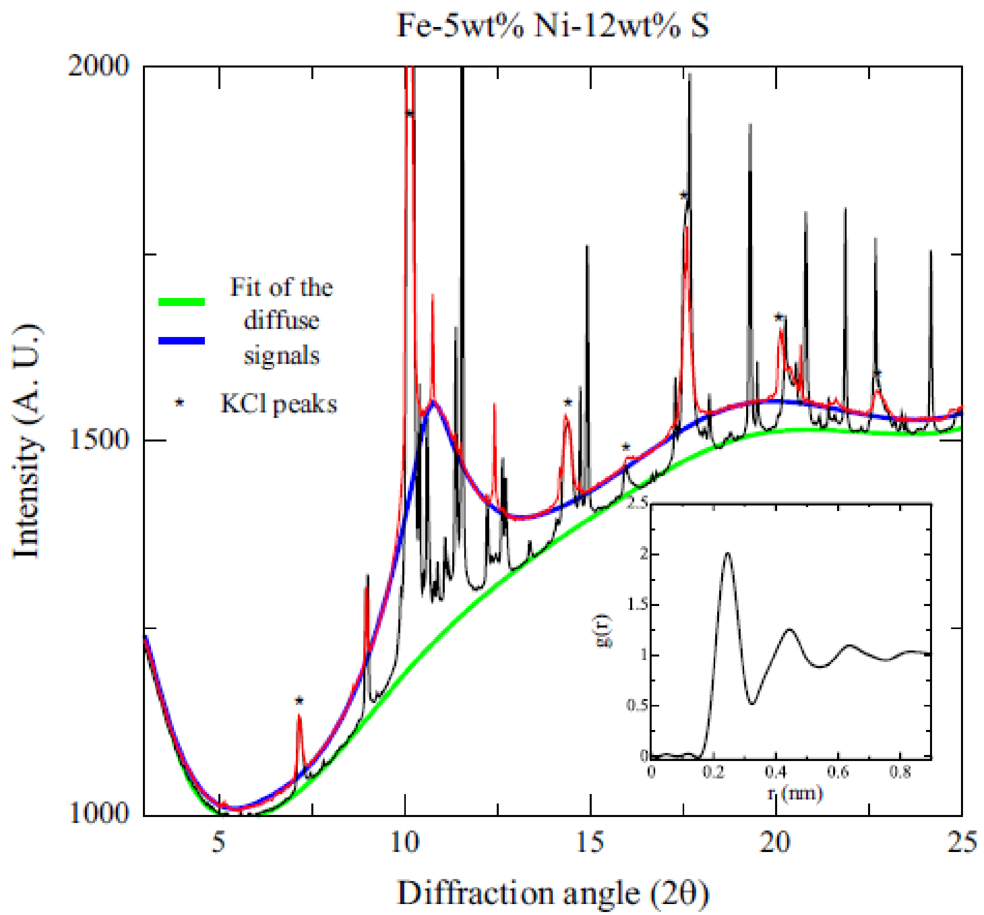

Composition of the Earth’s core

SEISMIC DATA

- Outer and inner core: 6-8% and 4-5% less dense than Fe
- 4-5 % P-wave velocity excess compared to Fe

GRAVITATIONAL FIELD

- Earth’s moment of inertia

COSMOCHEMISTRY

- Elements depleted in silicate Earth relative to chondrite meteorites
- Volatile elements

T_{IOCB} = 5400 – 6300 K
T_{CMB} = 4100 – 4300 K

% weight	Fe 55.85	Ni 58.69	S 32.07	Si 28.09	O 16.00	C 12.01	H 1.01
Liquid outer core	~85-90 %	~5 %	~1.7 %	~0-4 %	~0.8-5.3 %	~0.2 %	~0-0.3 %
Solid inner core	~90-93 %	~5 %	~0-1.1 %	~0-2.3 %	~0-0.1 %	~0-1.3 %	~0-0.2 %

[3] K. Hirose, B. Wood, L. Vocadlo. (2021) Nature Reviews Earth 2, 645–658

Upper to intermediate mantle

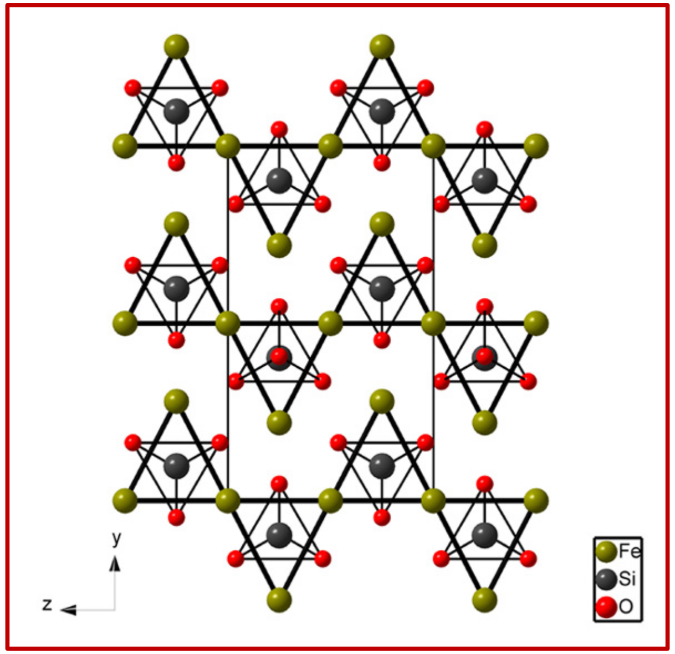

- Olivine: fayalite

$(Mg, Fe)_2^{[6]}\{^1{}_0\}[Si^{[4]\ulcorner 0;\, 0 \lrcorner}O_4]$

- Piroxene: enstatite, ferrosilite

$(Mg, Fe)_2^{[6]}\{^1{}_\infty\}[Si_2^{[4]\ulcorner 1;\, 2 \lrcorner}O_6]$

Exp.[12]
14.2 GPa
1600 K

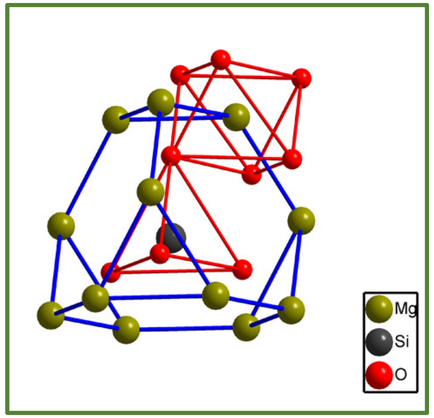

$(Mg, Fe)_6Si_3O_{12}$

- Spinel: ringwoodite, wadsleyite

$(Mg, Fe)_2^{[6]}\{^1{}_0\}[Si^{[4]\ulcorner 0;\, 0 \lrcorner}O_4]$

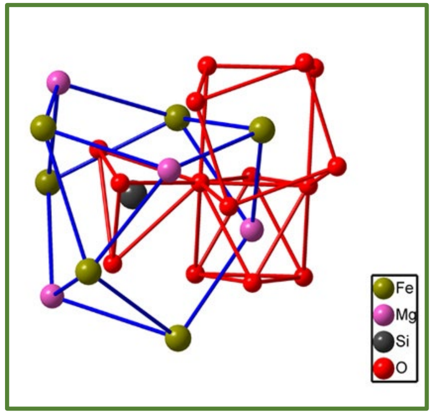

$(Mg, Fe)_5Si_3O_{12}$

- Garnet: skiagite

$(Mg, Fe)_3^{[8]}(Mg, Fe)_2^{[6]}\{^1{}_0\}[Si_3^{[4]\ulcorner 0;\, 0 \lrcorner}O_{12}]$

[12] T. Katsura *et al*. (2004) J. Geophys. Res. Solid Earth 109: B02209

Intermediate to lower mantle

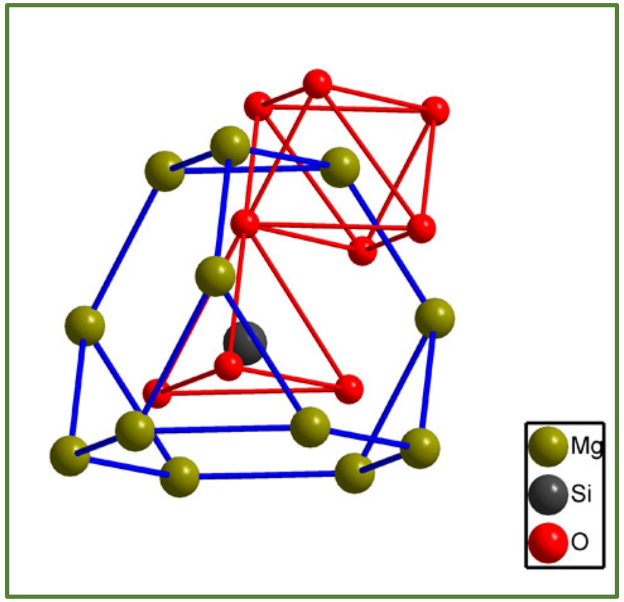

Exp.[13]
23 GPa
1600-2100 K

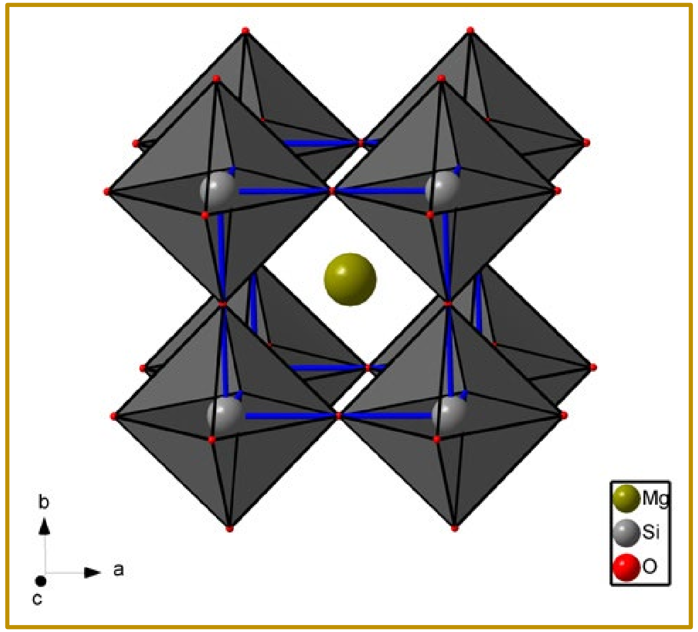

+ Periclase, magnesiowustite

(Mg, Fe)O

Spinel: ringwoodite, wadsleyite

$(Mg, Fe)_2^{[6]}\{^1{}_0\}[Si^{[4]\ulcorner 0;\, 0 \lrcorner}O_4]$

Perovskite

$(Mg, Fe)^{[12]}\{^3{}_\infty\}[Si^{[6]\ulcorner 1;\, 6 \lrcorner}O_3]$

[13] T. Katsura et al. (2003) Phys. Earth Planet. Inter. 136: 11-24

Lower mantle to D'' layer

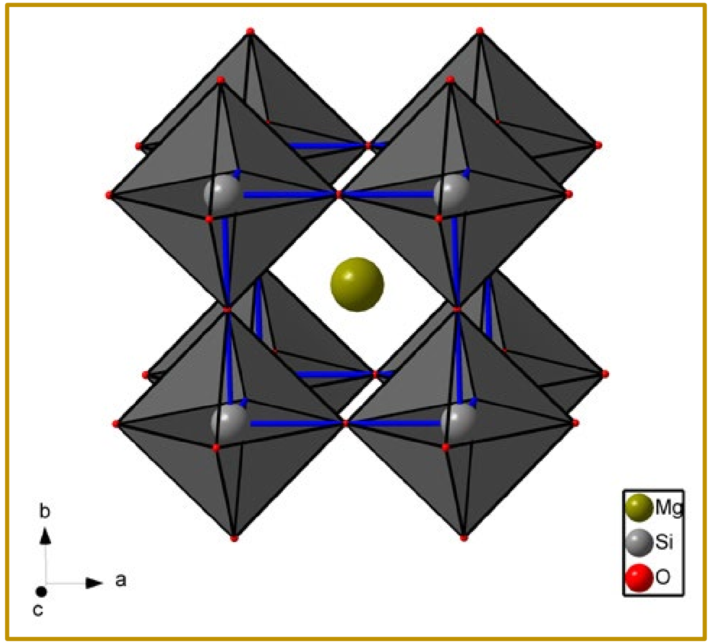

Perovskite

$(Mg, Fe)^{[8]}\{^{3}_{\infty}\}[Si^{[6]\lceil 1;\,6 \rfloor}O_3]$

Exp.[14]
> 125 GPa
> 2500 K

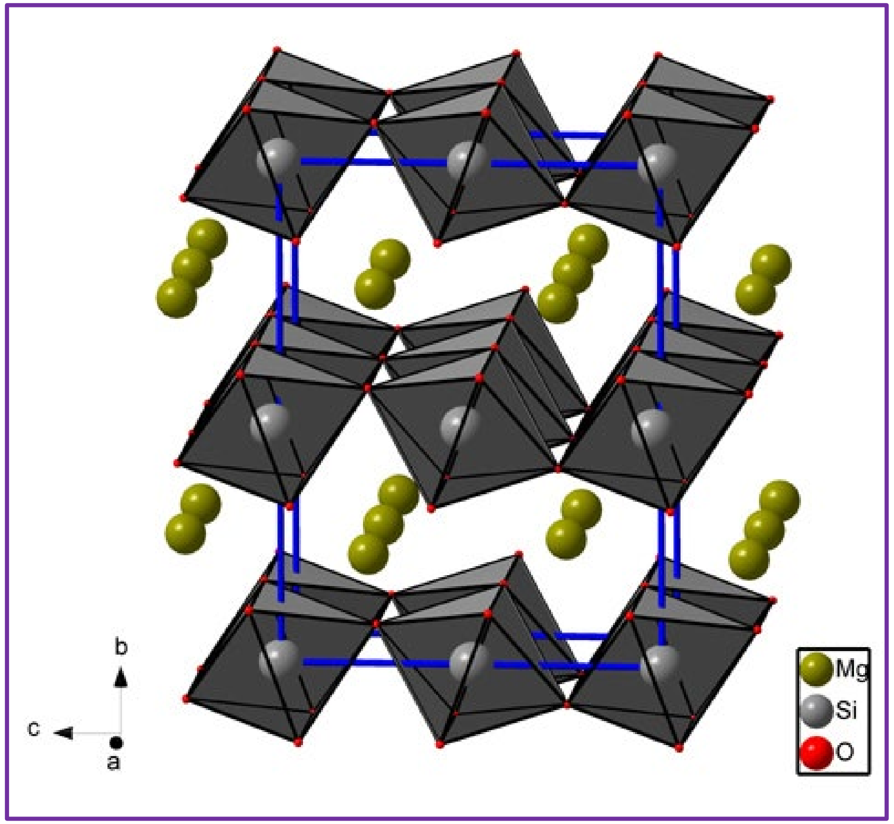

Post-perovskite

$(Mg, Fe)^{[8]}\{^{2}_{\infty}\}[Si^{[6]\lceil 1\text{-}2;\,4 \rfloor}O_3]$

[14] M. Murakami et al. (2004) Science 304: 855-858

Silicate-carbonate cycle / Deep carbon cycle

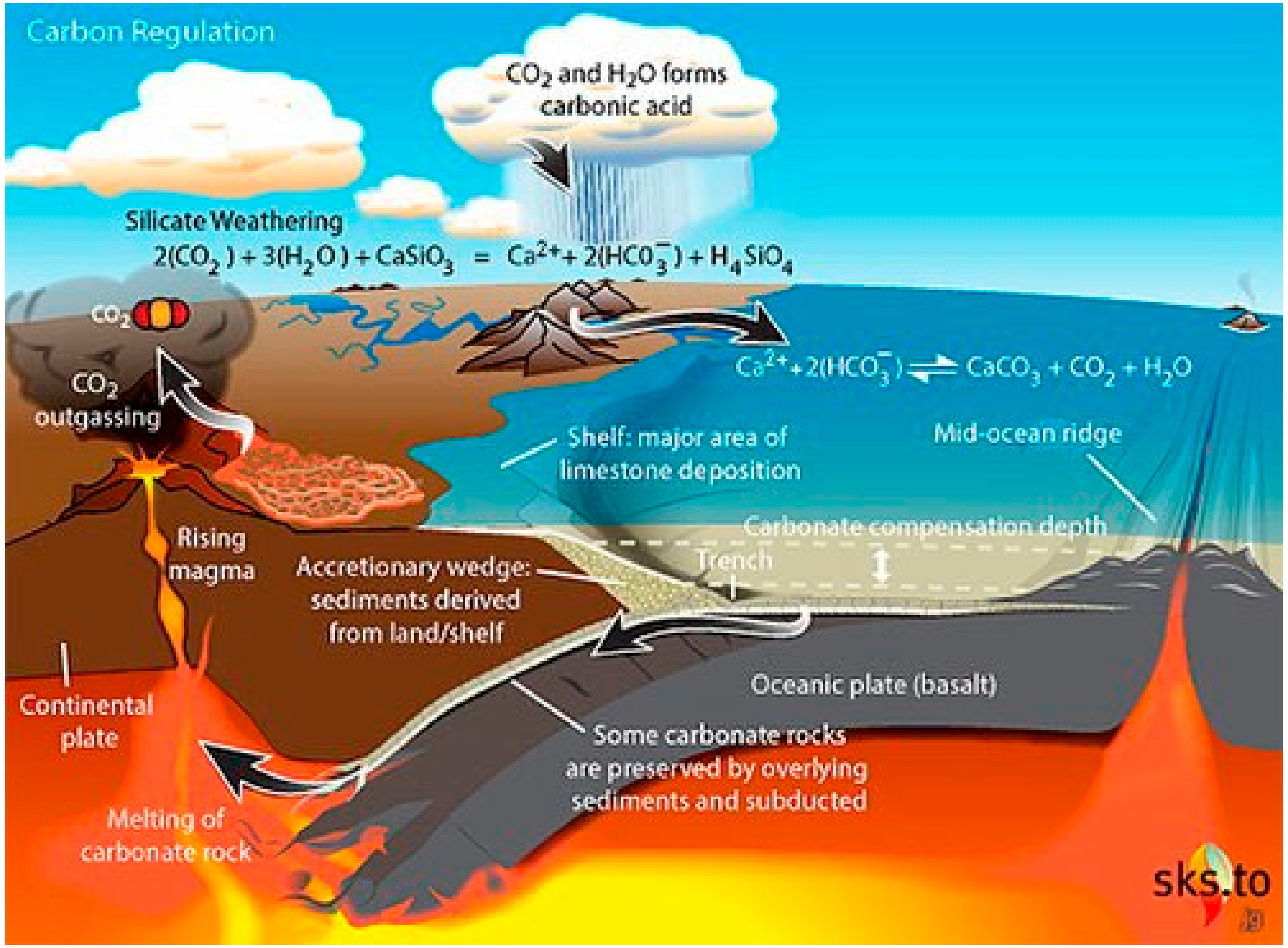

[15] R. Dasgupta (2013) Rev. Mineral Geochem. 75, 183.

WEATHERING

- Carbonic acid reacts with silicate minerals → CARBONATES

WATER CYCLE

- Interconnection

CLIMATE STABILIZATION

- Geological Eras

METAMORPHISM REACTIONS / VULCANISM

- Formation of silicates + CO_2

CARBON RESERVOIR

- Carbonates at great depths

Phase behavior and polymorphism (Example 1: Barytocalcite, $BaCa(CO_3)_2$)

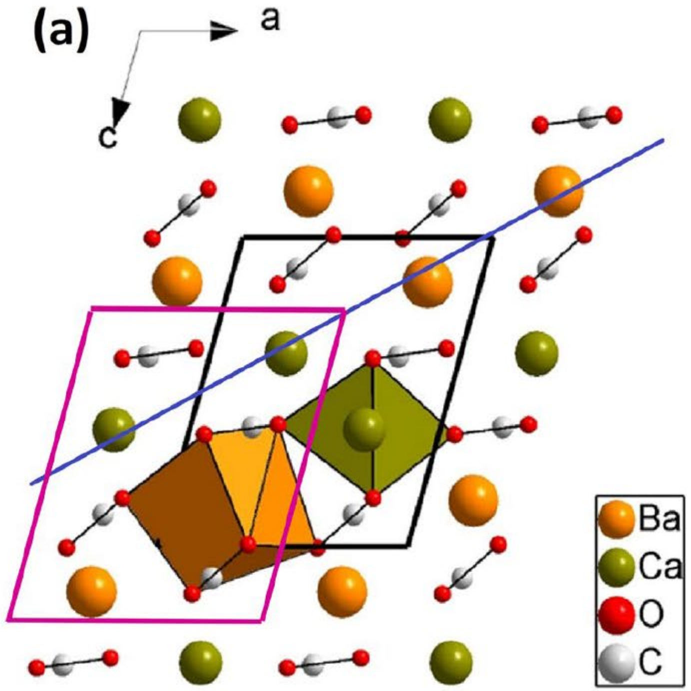

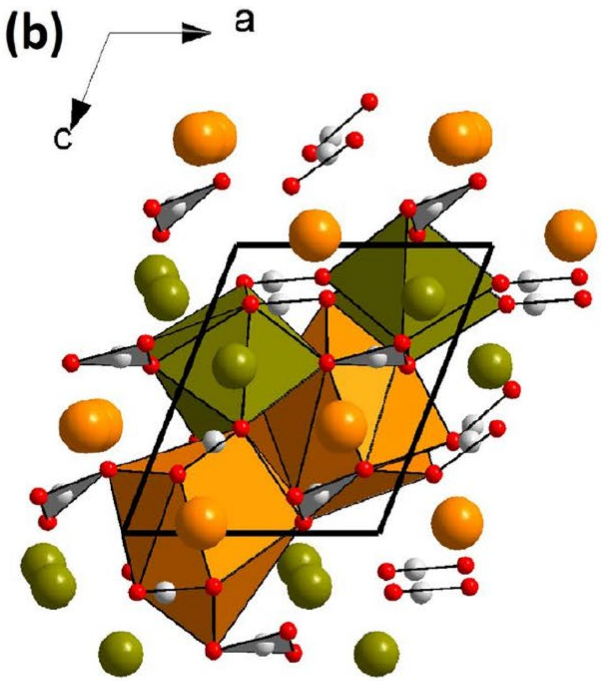

Barytocalcite → **Post-barytocalcite**

5.7 GPa

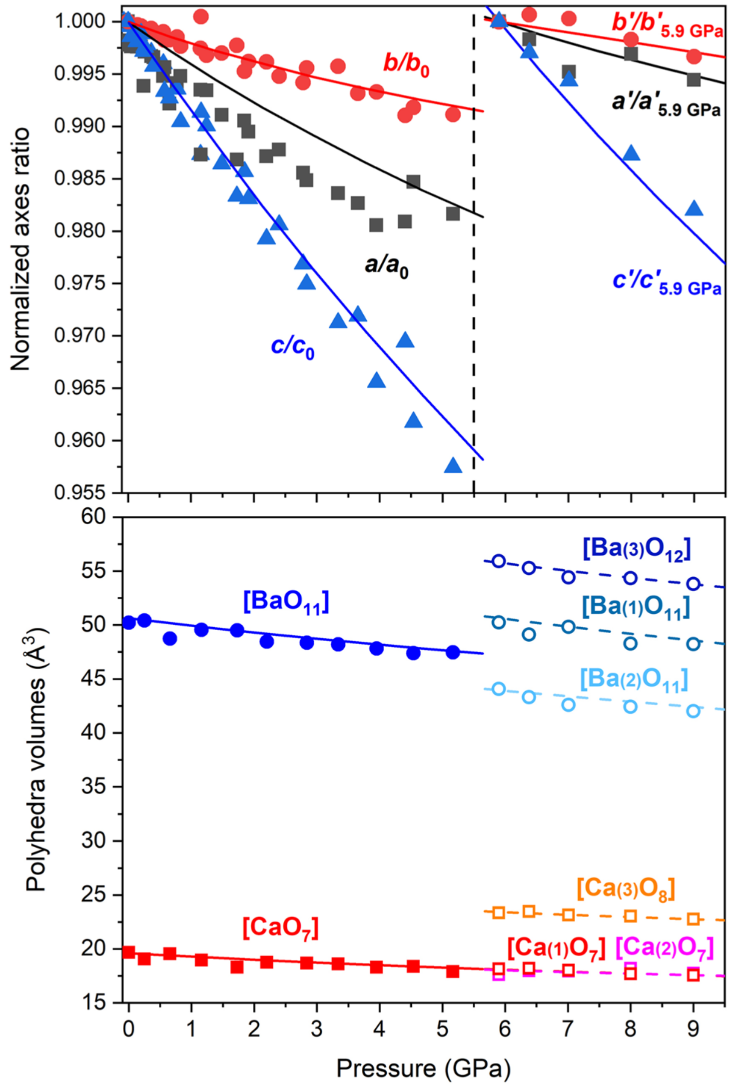

[16] R. Chuliá-Jordán et al. (2022) Sci. Rep. 12, 7413.

Phase behavior and polymorphism (Example 2: Nesquehonite, $MgCO_3 \cdot 3H_2O$)

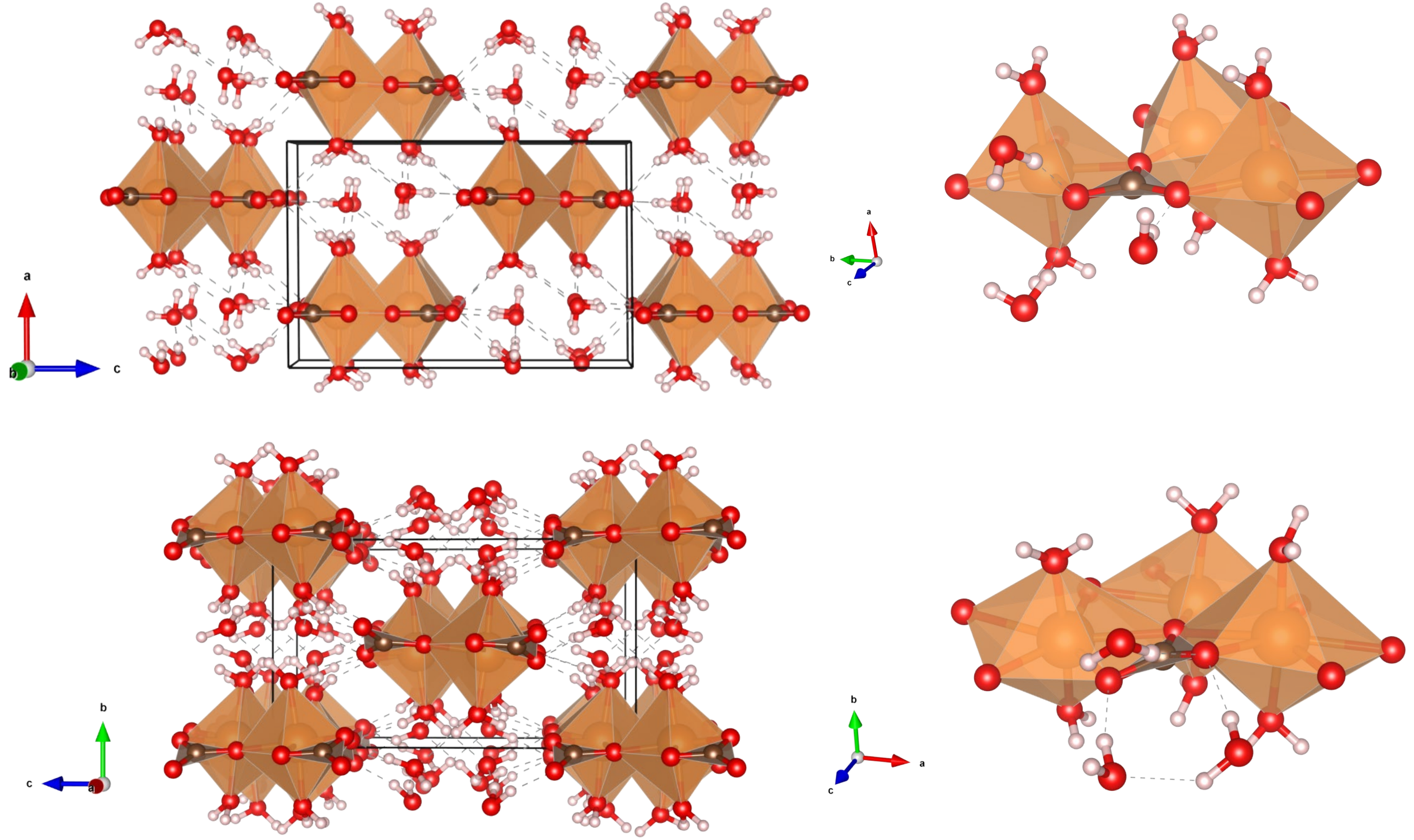

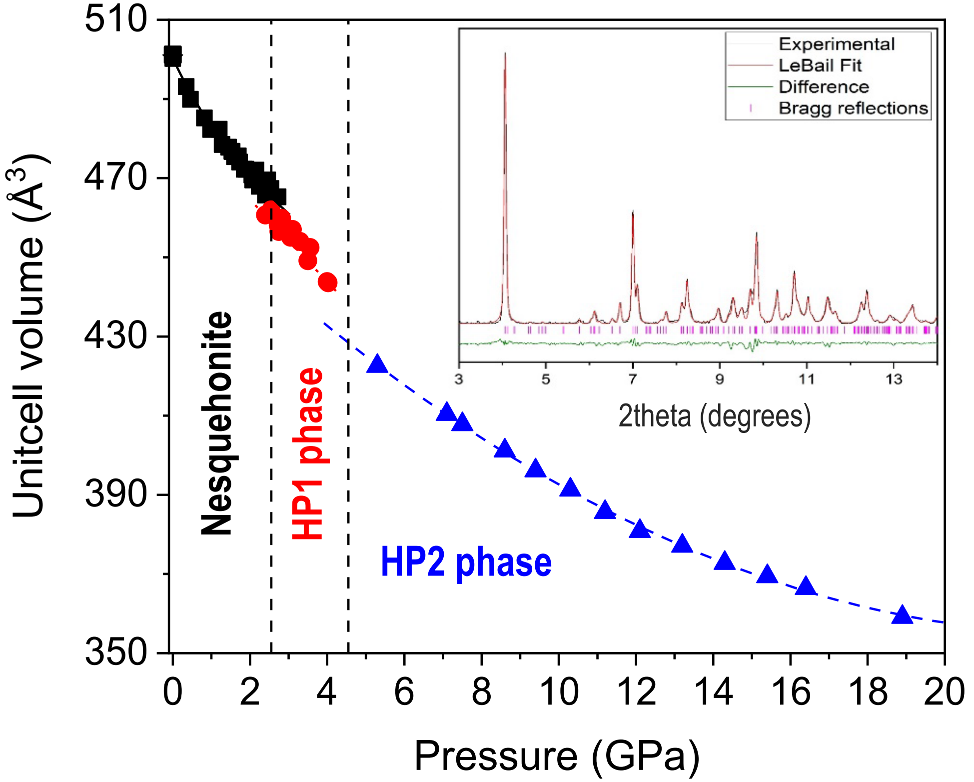

[17] D. Santamaria-Perez et al. (2024) Cryst. Growth Des. 24, 1159.

[18] B.D. Botan-Neto et al. (2024) Inorg. Chem. 63. 12, 15762.

Diamond formation

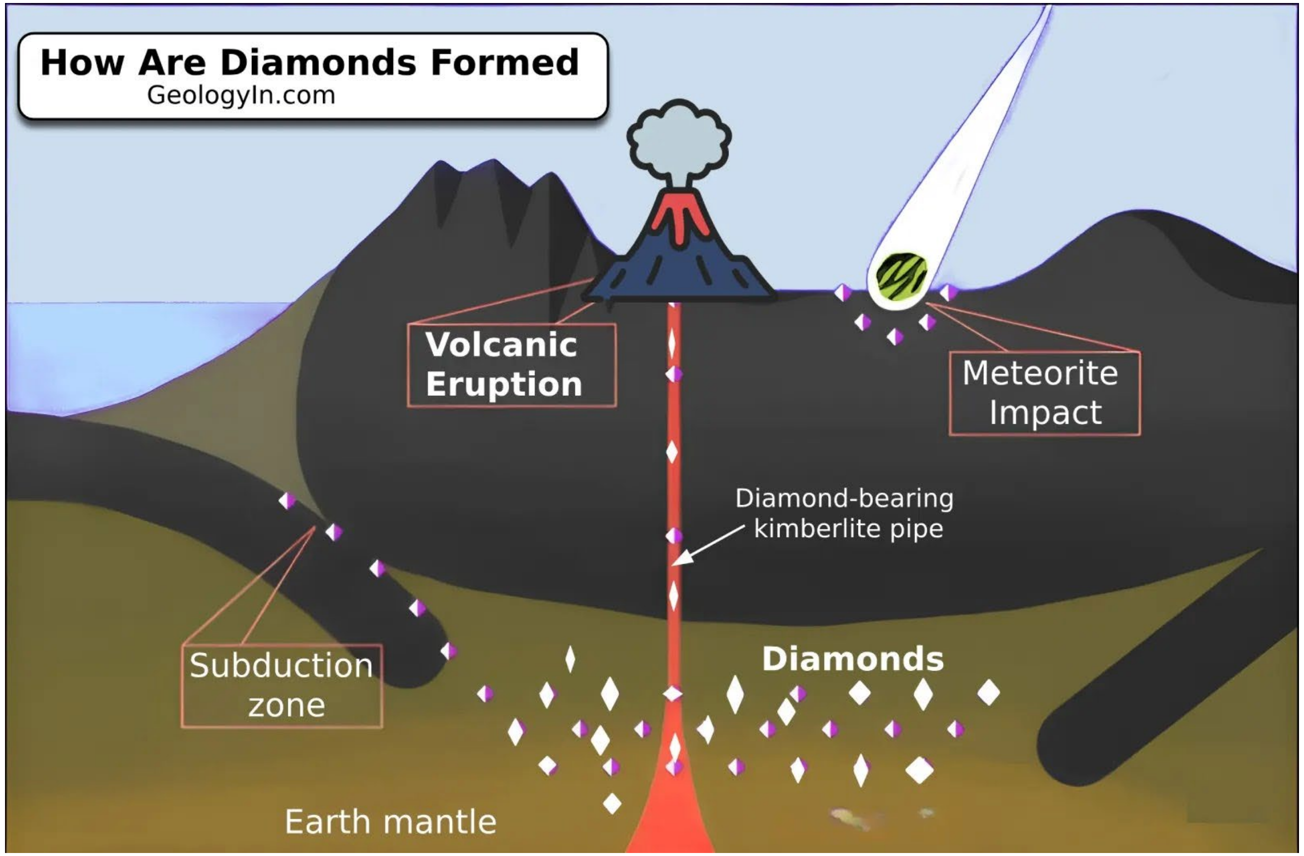

$$6\left(Fe_{2/3}Mg_{1/3}\right)^{2+}CO_3 \rightarrow 2MgFe_2^{3+}O_4 + C\,(diamond) + 5CO_2.$$

Experimental results

Self-redox of ferromagnesian carbonate

- Reduction of carbon
- Pressures and temperatures to cross the graphite–diamond transition boundary

(P > 25 GPa y T > 800ºC)

[19] M. Chen et al. (2018) PNAS, 115, 2676

Silicate-carbonate phases at extreme conditions

Tilleyite $Ca_5(Si_2O_7)(CO_3)_2$

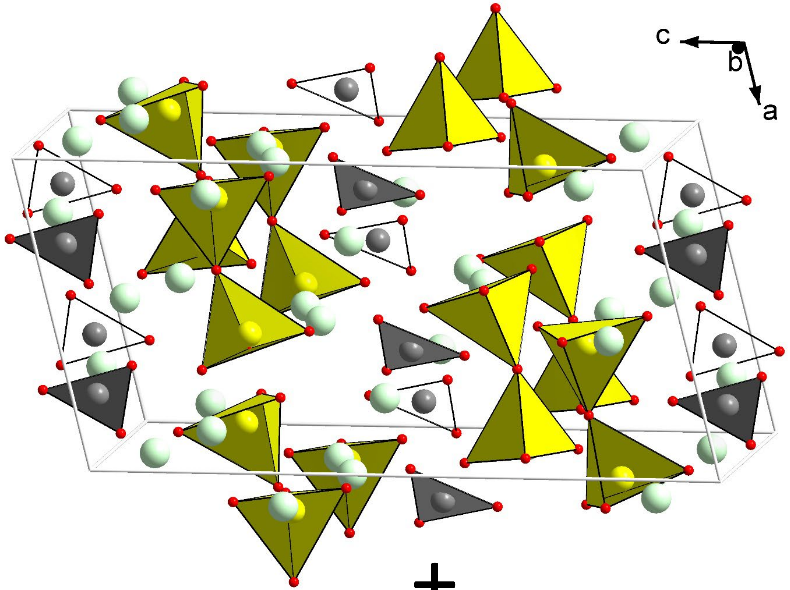

+

CO_2

P = 39.5 GPa
T = 2600 K

$Ca_2Si(CO_3)_4$

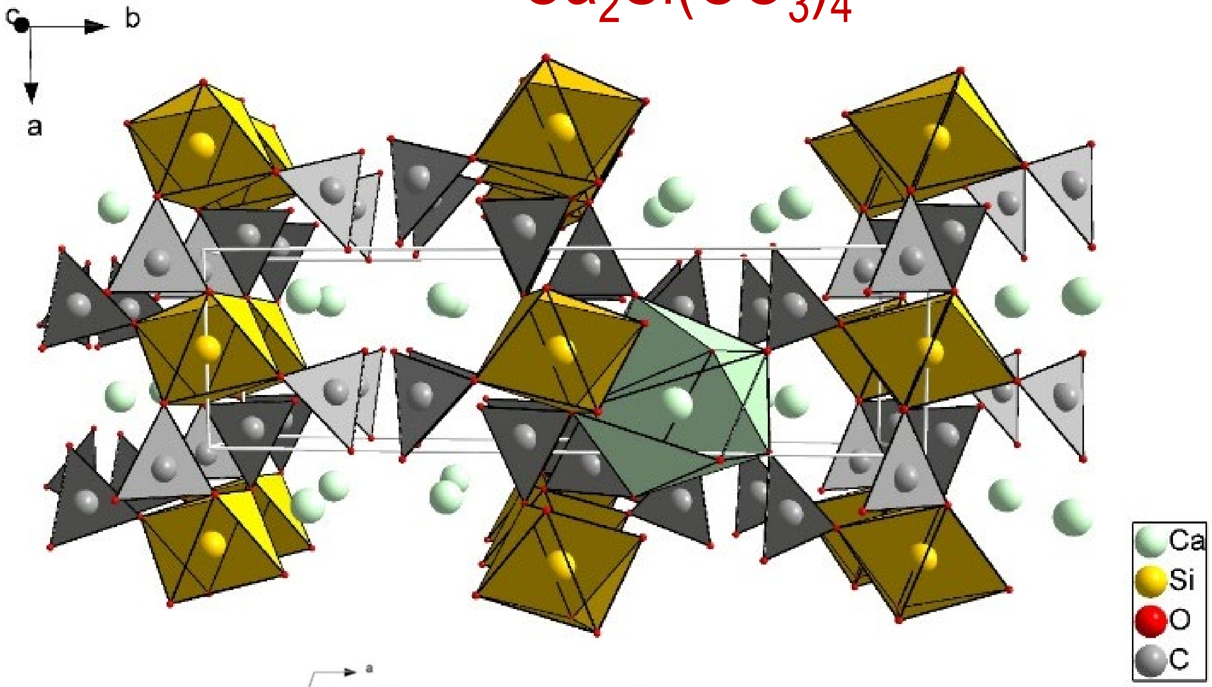

+

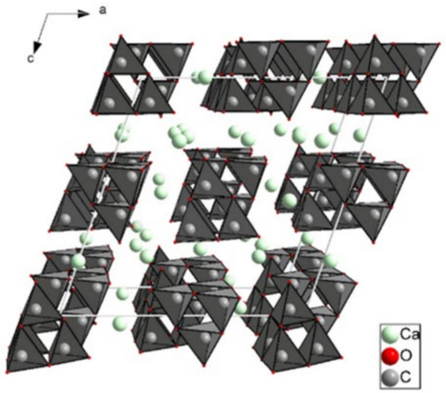

$Ca_2C_4O_{10}$

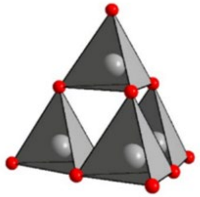

[20] D. Santamaria-Perez et al. (2019) Sci. Rep. 9, 7898.
[21] B.D. Botan-Neto, et al (2026) Angew. Chem. Int. Ed. 65, e24999

Metallization of hydrogen by shock compression

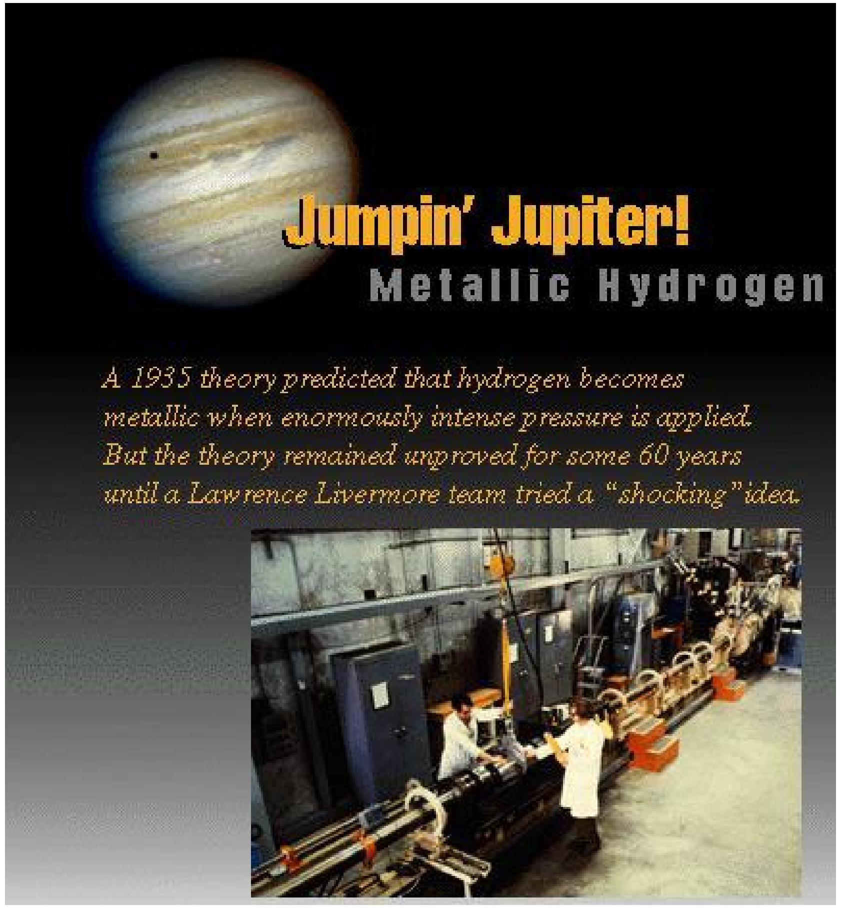

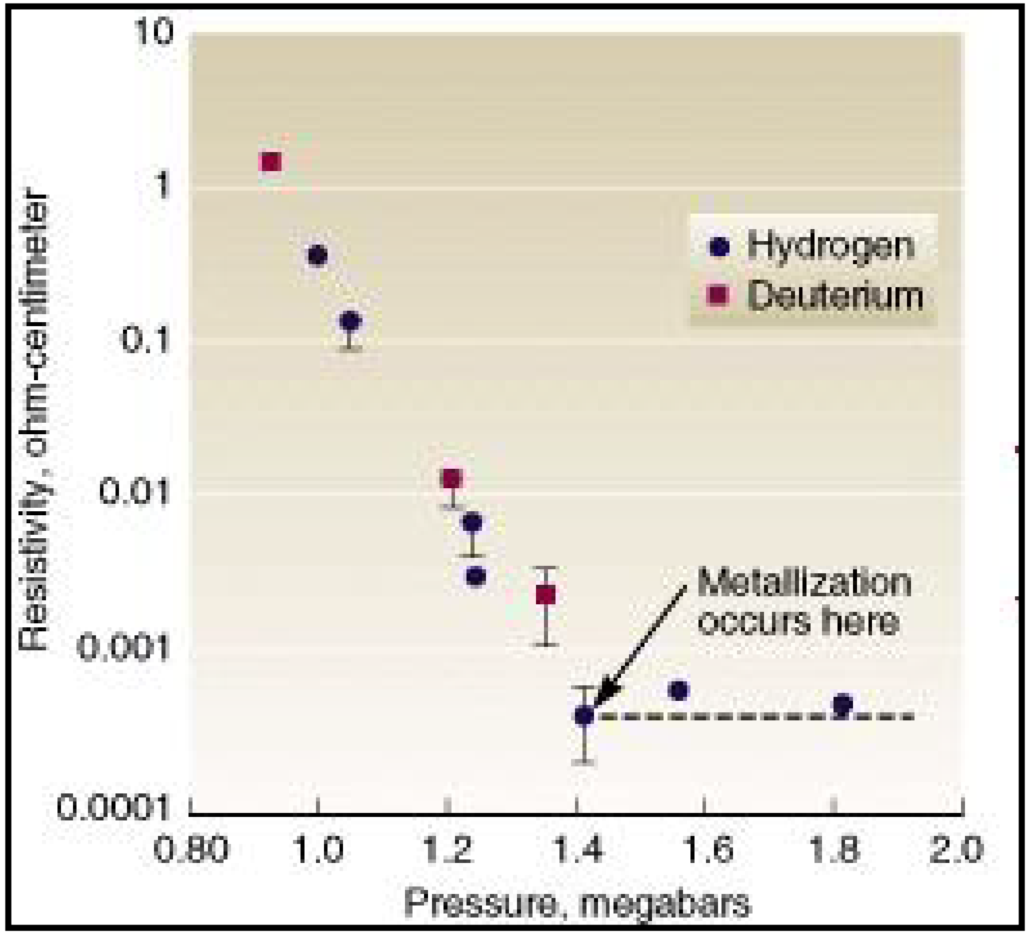

[Z] E. Wigner, H.B. Huntington (1935) J. Chem. Phys. 3, 764

[Z] N.W. Ashcroft (1968) Phys. Rev. Lett. 21, 1748

[Y] W.J. Nellis, S.T. Weir, A.C. Mitchell (1996) Science 273, 936

Phase diagram and Equation of state of H_2 and D_2 from X-ray diffraction

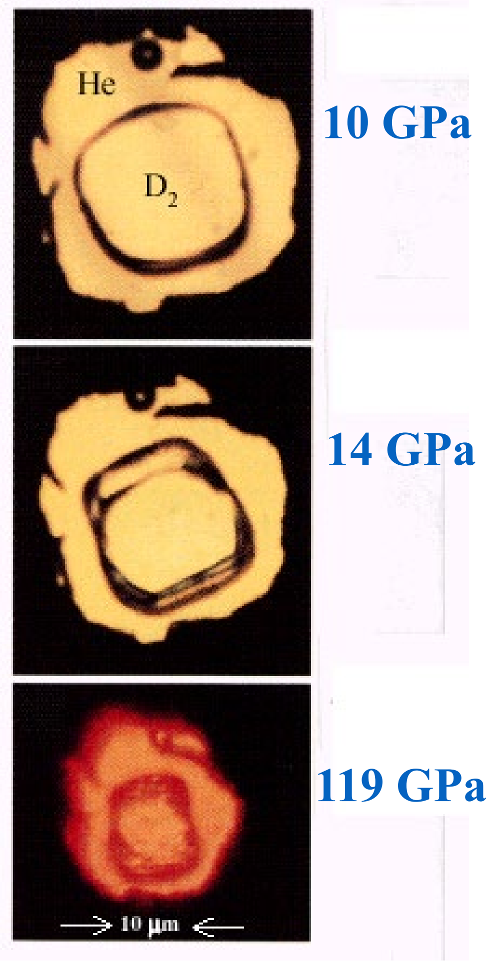

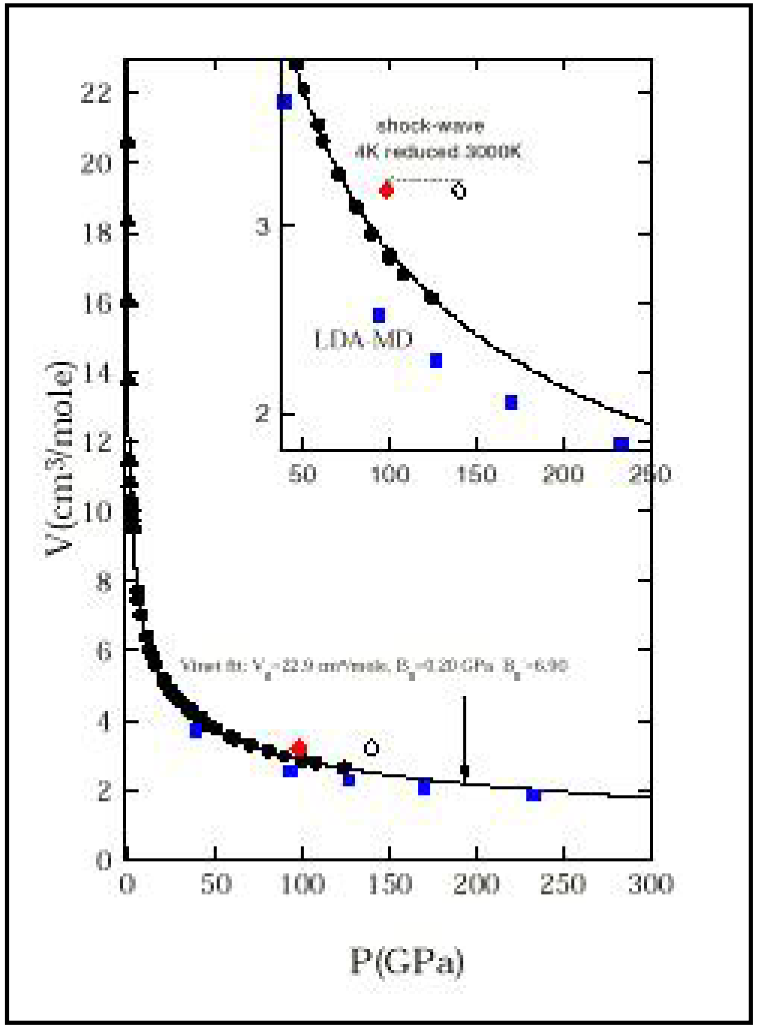

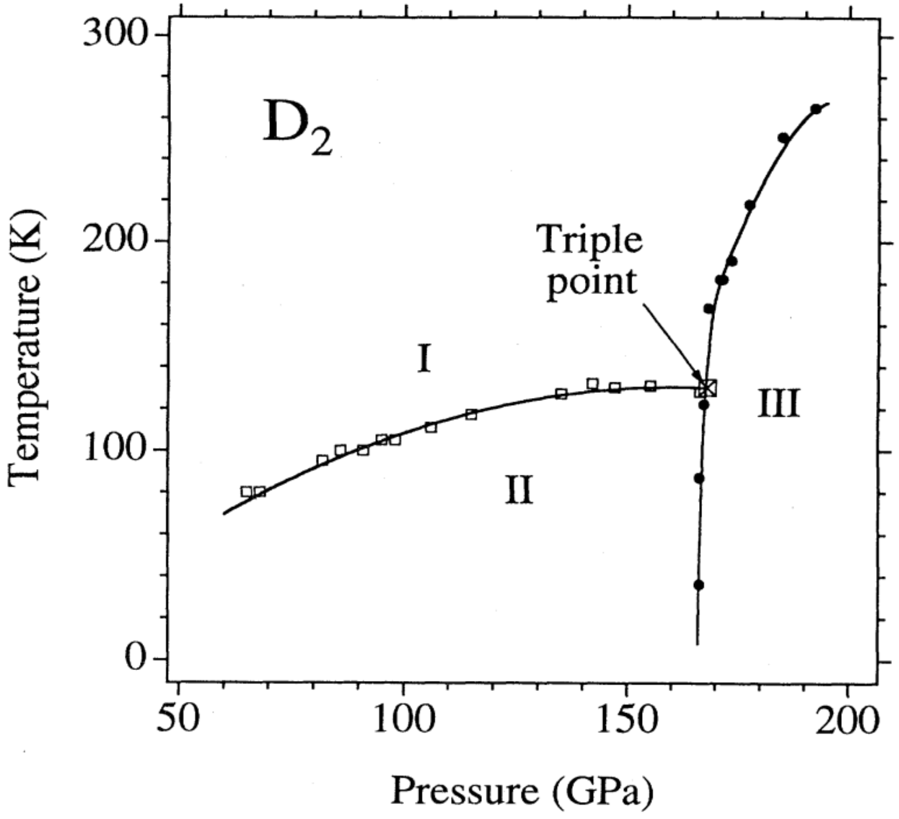

[X] P. Loubeyre, et al. (1996) Nature 383, 702
[X] H.K. Mao, R. Hemley (1994) Rev. Modern Phys. 66, 671

Literature on Metallization of hydrogen (HOT TOPIC)

1. Pickard, C. J. & Needs, R. J. Structure of phase III of solid hydrogen. *Nat. Phys.* **3**, 473–476 (2007).
2. McMahon, J. M., Morales, M. A., Pierleoni, C. & Ceperley, D. M. The properties of hydrogen and helium under extreme conditions. *Rev. Mod. Phys.* **84**, 1607–1653 (2012).
3. Monserrat, B. et al. Structure and metallicity of phase V of hydrogen. *Phys. Rev. Lett.* **120**, 255701 (2018).
4. Monacelli, L., Casula, M., Nakano, K., Sorella, S. & Mauri, F. Quantum phase diagram of high-pressure hydrogen. *Nat. Phys.* **19**, 845–850 (2023).
5. Hazen, R. M., Mao, H. K., Finger, L. W. & Hemley, R. J. Single-crystal x-ray diffraction of *n*-H_2 at high pressure. *Phys. Rev. B* **36**, 3944–3947 (1987).
6. Ginzburg, V. L. Nobel Lecture: on superconductivity and superfluidity (what I have and have not managed to do) as well as on the "physical minimum" at the beginning of the XXI century. *Rev. Mod. Phys.* **76**, 981–998 (2004).
7. Ashcroft, N. W. Metallic hydrogen: a high-temperature superconductor?. *Phys. Rev. Lett.* **21**, 1748–1749 (1968).
8. Wigner, E. & Huntington, H. B. On the possibility of a metallic modification of hydrogen. *J. Chem. Phys.* **3**, 764 (1935).
9. Mao, H. K. et al. Synchrotron X-ray diffraction measurements of single-crystal hydrogen to 26.5 gigapascals. *Science* **239**, 1131–1134 (1988).
10. Loubeyre, P. et al. X-ray diffraction and equation of state of hydrogen at megabar pressures. *Nature* **383**, 702–704 (1996).
11. Eremets, M. I., Drozdov, A. P., Kong, P. P. & Wang, H. Semimetallic molecular hydrogen at pressure above 350 GPa. *Nat. Phys.* **15**, 1246–1249 (2019).
12. Loubeyre, P., Occelli, F. & Dumas, P. Synchrotron infrared spectroscopic evidence of the probable transition to metal hydrogen. *Nature* **577**, 631–635 (2020).
13. Goncharenko, I. & Loubeyre, P. Neutron and X-ray diffraction study of the broken symmetry phase transition in solid deuterium. *Nature* **435**, 1206–1209 (2005).
14. Akahama, Y. et al. Evidence from x-ray diffraction of orientational ordering in phase III of solid hydrogen at pressures up to 183 GPa. *Phys. Rev. B* **82**, 060101 (2010).
15. Ji, C. et al. Ultrahigh-pressure isostructural electronic transitions in hydrogen. *Nature* **573**, 558–562 (2019).
16. Mao, H.-k. & Hemley, R. J. Ultrahigh-pressure transitions in solid hydrogen. *Rev. Mod. Phys.* **66**, 671–692 (1994).
17. Eremets, M. I. & Troyan, I. A. Conductive dense hydrogen. *Nat. Mater.* **10**, 927–931 (2011).
18. Howie, R. T., Guillaume, C. L., Scheler, T., Goncharov, A. F. & Gregoryanz, E. Mixed molecular and atomic phase of dense hydrogen. *Phys. Rev. Lett.* **108**, 125501 (2012).
19. Howie, R. T., Scheler, T., Guillaume, C. L. & Gregoryanz, E. Proton tunneling in phase IV of hydrogen and deuterium. *Phys. Rev. B* **86**, 214104 (2012).
20. Dalladay-Simpson, P., Howie, R. T. & Gregoryanz, E. Evidence for a new phase of dense hydrogen above 325 gigapascals. *Nature* **529**, 63–67 (2016).
21. Mazin, I. I., Hemley, R. J., Goncharov, A. F., Hanfland, M. & Mao, H.-k Quantum and classical orientational ordering in solid hydrogen. *Phys. Rev. Lett.* **78**, 1066–1069 (1997).
22. Nagara, H. & Nakamura, T. Stable phases of solid hydrogen at megabar pressures and at zero temperature. *Phys. Rev. Lett.* **68**, 2468–2471 (1992).
23. Natoli, V., Martin, R. M. & Ceperley, D. Crystal structure of molecular hydrogen at high pressure. *Phys. Rev. Lett.* **74**, 1601–1604 (1995).
24. Johnson, K. A. & Ashcroft, N. W. Structure and bandgap closure in dense hydrogen. *Nature* **403**, 632–635 (2000).
25. Kitamura, H., Tsuneyuki, S., Ogitsu, T. & Miyake, T. Quantum distribution of protons in solid molecular hydrogen at megabar pressures. *Nature* **404**, 259–262 (2000).
26. Ji, Ch., ..., H.K. Mao. Ultrahigh-pressure crystallographic passage towards metallic hydrogen. *Nature* **641**, 904-909 (2025).
27. Dias, R.P., Silvera, I.F. Observation of the Wigner-Huntington transition to metallic hydrogen. Science 355, 715-718 (2017)

Conclusions

- ✓ High-pressure and high-temperature techniques make it possible to reproduce the thermodynamic conditions of the Earth's geotherm and those of other planetary bodies, while simultaneously enabling the in situ characterization of representative samples. This approach yields key insights into the structure, composition, and evolution of planets.

The results both complement and are constrained by evidence from other disciplines, including seismology, gravitational modelling, and heat-transfer studies.

- ✓ Despite remarkable progress over recent decades, much remains to be discovered about the Earth's interior. Numerous fundamental questions are still unresolved, offering exciting opportunities for future research.

Acknowledgments

Funding Projects

CIAICO/2021/241

MFA/2022/007

CIGRIS/2022/202

CIBEST/2022/198

MCIN/AEI/10.13039/501100011033

PID2021-125518NB-I00

PID2024-158791NB-I00

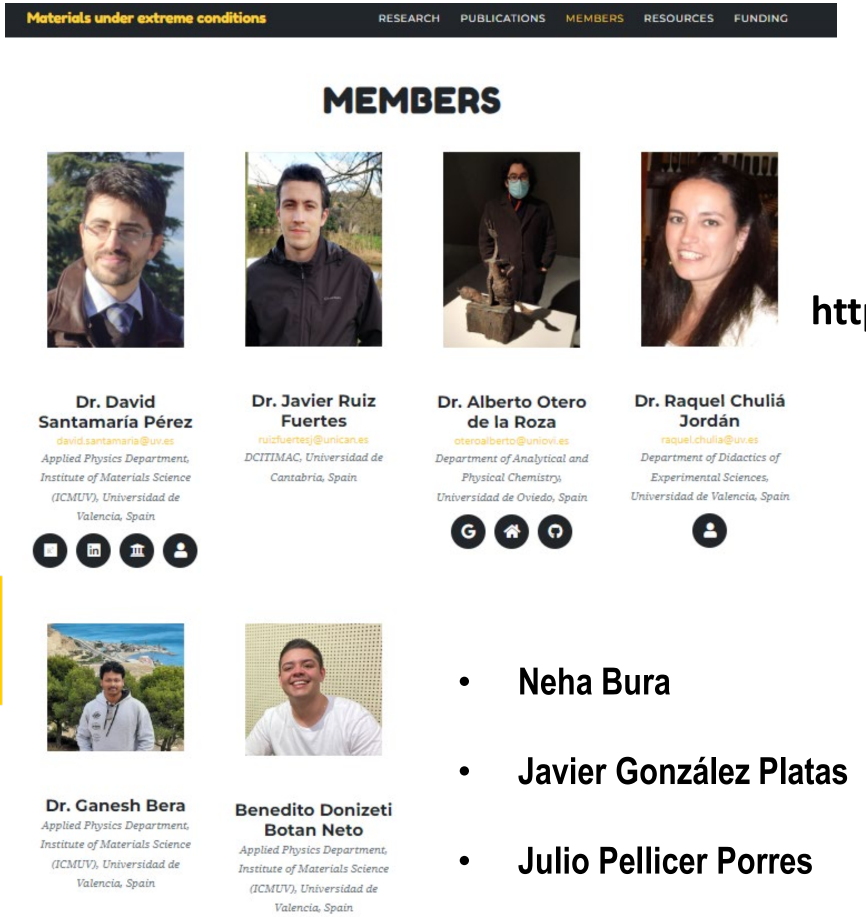

- Neha Bura
- Javier González Platas
- Julio Pellicer Porres

https://extreme-carbonates.github.io/

Thank You!

E-mail: David. Santamaria@uv.es